AALTO UNIVERSITY
SCHOOL OF SCIENCE AND TECHNOLOGY
Department of Communications and Networking (Comnet)

Beneyam Berehanu Haile

Co-channel Interference in Heterogeneous Networks: Rician/Rayleigh Scenario

Master's Thesis submitted in partial fulfilment of the requirements for the degree of Master of Science in Technology.

Helsinki, September 17, 2010

Supervisor: Professor Jyri Hämäläinen

Instructor: M.Sc. (Tech.) Taneli Riihonen

AALTO UNIVERSITY ABSTRACT OF THE
SCHOOL OF SCIENCE AND TECHNOLOGY MASTER'S THESIS

Author:	Beneyam Berehanu Haile	
Name of the Thesis:	Co-channel Interference in Heterogeneous Networks: Rician/Rayleigh Scenario	
Date:	September 17, 2010	**Number of pages:** 68
Department:	Department of Communications and Networking	
Professorship:	S-72	
Supervisor:	Prof. Jyri Hämäläinen	
Instructor:	M.Sc. (Tech.) Taneli Riihonen	

The purpose of this study is to analyze interference for a macrocellular network which embeds femtocells and/or relay nodes. Femtocells and relay nodes are being introduced to improve coverage and capacity of conventional cellular networks. However, their introduction comes with additional interference between the macrocell and femtocell/relay node, and between individual femtocells/relay nodes. Hence, there is a need for analytical expressions for the performance measures such that outage probability and average capacity so that the effect of co-channel interference is understood thoroughly. In this thesis, analytical and numerical results are presented for outage probability and average capacity in a Rician/Rayleigh Scenario. In this scenario, the desired signal experiences Rician fading channel and the interfering signals experience Rayleigh fading channels. Closed-form and infinite series expressions are found for the outage probability and an infinite sum expression is found for the average capacity. The analysis approximates SINR by its tight upper bound SIR; therefore, the outage probability result is a tight lower bound and the average capacity result is a tight upper bound of their corresponding results without the approximation. Moreover, the thesis, as a background work, includes detailed studies of the relevant probability distributions used to model fading channels and radio link performance metrics in the absence of interference.

Keywords: Probability Distributions, Channel Modeling, Co-channel Interference, Rayleigh Fading, Rician Fading, Nakagami Fading, Weibull Fading, Log-normal Fading, Outage Probability, Outage Capacity, Average Capacity, Heterogeneous Networks

Acknowledgements

This work was carried out at the Department of Communications and Networking at Aalto University as a part of Advances in Wireless Access project funded by TEKES, Nokia Siemens Networks and Ericsson. There are people to whom I own a debt of gratitude for making the course of my research both an enriching and an enjoyable experience.

Firstly I wish to express my sincerest thanks to my supervisor, Professor Jyri Hämäläinen, for the enthusiastic guidance and encouragement he has given me throughout the thesis work. He showed me the path and smoothed my journey but I am grateful that he also showed me the freedom to explore as I desired.

I am also honored to have been able to work with my instructor, M.Sc. Taneli Riihonen. His advice and assistance has been appreciated. I hope to continue working with him.

I acknowledge the support of my friends Emma Jokinen and Tenager Bekalu.

Finally I must thank my family, and especially my mother, who have given me a lifetime of loving support and encouragement.

Otaniemi, September 17, 2010

Beneyam Berehanu Haile

Contents

List of Abbreviations

OFDM	Orthogonal Frequency Division Multiplexing
AWGN	Additive White Gaussian Noise
LTV	Linear Time Variant
LTI	Linear Time Invariant
PDF	Probability Density Function
CDF	Cumulative Distribution Function
MGF	Moment Generating Function
CF	Characteristic Function
BEP	Bit Error Probability
SEP	Symbol Error Probability
BLER	Block Error Rate
PSK	Phase Shift Keying
BPSK	Binary Phase Shift Keying
CCI	Co-channel Interference
LOS	Line-of-Sight
NLOS	Non-Line-of-Sight
BW	Bandwidth

SINR	Signal-to-Interference-Noise Ratio
SIR	Signal-to-Interference Ratio
SNR	Signal-to-Noise Ratio

List of Notations

$\triangleq$	defined as equal to ($a \triangleq b$: a is defined as b)
$f_X(x)$	Probability Density Function of Random Variable X
$F_X(x)$	Cumulative Function of Random Variable X
$M_X(s)$	Moment Generating Function of Random Variable X
$\phi_X(w)$	Characterstic Function of Random Variable X
E[X]	Expected Value of Random Variable X
μ_X	Mean of a Random Variable X
VAR[X]	Variance of Random Variable X
$P\{z\}$	The Probability of an Event z
h_c	Complex Baseband Channel
h	Amplitude of h_c
γ	Signal-to-Interference-Plus-Noise Ratio
$\tilde{\gamma}$	Signal-to-Interference Ratio
$\bar{\gamma}_i$	Average of Random Variable γ_i
K	Rician K factor
P_b	Instantaneous BEP
$\bar{P}_b$	Average BEP

P_{out}	Outage Probability
ϵ	Quality of Service Requirement
C	Average Capacity
S	The Sum of M Exponentially Distributed Random Variable
P'_{out}	Outage Probability for Multi-interferer Scenario
C'	Average Capacity for Multi-interferer Scenario

List of Figures

List of Tables

Chapter 1

Introduction

Future networks are expected to offer significantly improved coverage and capacity. Embedding small base stations in a macro-cellular network appears to be one of the most promising techniques for desired coverage and capacity improvement for all users including those around the cell edge. On the other hand, carrier frequencies allocated for the networks are high and hence vulnerable to severe radio propagation losses, especially at the cell edge. Thus, to meet the coverage and capacity requirements of the networks under the conventional cellular network architectures, there is a need to increase the density of base stations significantly, which result in high deployment cost that could not be accepted by operators. Therefore, small cells, relay nodes and femtocells, are being considered as cost-effective solutions to meet the requirements. Networks with co-channel deployment of different types of base stations are referred to as heterogeneous networks.

In heterogeneous network, interference between macrocell and femtocell/relay node, as well as between individual femtocells/relay nodes, is one of the major challenges. Analytical expressions for different radio link performance measures are important since they can be used to investigate the effects of co-channel interference theoretically. Generating and discussing analytical expressions for the widely used radio link performance measures is the primary aim of this thesis. As objectives, two key research questions will be addressed in this work:

1. What is the probability of a given node in a radio link of a heterogeneous

network be out of a given quality of service?

This question will be addressed by producing expressions for a measure called the outage probability.

2. What is the largest average transmission rate that can be achieved in a given radio link within a heterogeneous network?

   This question will be addressed by producing expression for a measure called the average capacity.

There are many research works which have analyzed the effects of co-channel interference in different fading channel models for both macrocellular and microcellular mobile radio systems. Most of the works for macrocellular systems have assumed the same statistical fading channel model for the desired signal and interfering signals; whereas, most of the works for microcellular systems have assumed different statistical models for the desired signal's channel and interfering signals' channels. Furthermore, almost all the works for both systems have performed the analysis in terms of only one of the key radio link performance measure, namely outage probability. In this thesis work, the focus is on interference for a heterogeneous network with in a fading environment scenario that is common in presence of femtocells and relay nodes, namely Rician/Rayleigh. In this scenario, the desired signal and the interfering signals subjected to different statistical channel models such that Rician fading channel for the desired signal and Rayleigh fading channels for the interfering signals. We present a detailed analysis and discussion on outage probability and average capacity for the Rician/Rayleigh scenario.

The research methods which are used in this thesis are literature review, and mathematical and numerical analysis with the help of Mathematica, Matlab, and tables and handbooks of integrals, series, and special functions. The literature review is conducted to get the overall understanding of statistical fading channel models, performance measures in fading channels and previous studies on co-channel interference. Statistical probability distributions used to model fading channels are studied in detail. These distributions are Gaussian, chi-square, Rayleigh, Rician, lognormal, Nakagami, and Weibull. Furthermore, the thesis includes a detailed analysis and discussion of average

bit error probability (BEP), outage probability, and average capacity in the absence of interference.

The rest thesis is structured as follows:

- *Chapter 2* deals with the radio link model used in the thesis. It discusses the basic concepts, mainly wireless linear time-invariant channels, and assumptions required to formulate a suitable link model.
- *Chapter 3* discusses the characterization and application of probability distributions which are relevant to model fading channels. Furthermore, the different statistical fading channel models are described in detail.
- *Chapter 4* analyzes and discusses radio link performance measures for fading channels in the absence of co-channel interference. The key performance measures which are considered in the analysis are average BEP, outage probability, and average capacity.
- *Chapter 5* presents analysis of outage probability and average capacity for the Rician/Rayleigh fading environment scenario. First the analysis will be made for a single interferer scenario, and then there will be an extension to multi-interferer situations.
- *Chapter 6* concludes the thesis work by pointing out its accomplishments and recommends further extensions for the research.

Chapter 2

Link Level Signal Model

The purpose of this chapter is to give a brief discussion on a digital communication link-level signal model that is used throughout this thesis.

2.1 Communication System Model

Figure 2.1 shows the block diagram of a conceptual communication system that is usually employed in the mathematical analysis of information transmission. The model is introduced by C. E. Shannon, the father of information theory, in the mid 20^{th} century. It comprises blocks denoting information source and sink, designed transmitter and receiver, and transmission channel. The information required to be transmitted successfully to the information sink is generated at the information source. The transmitter and the receiver are digital signal processors that are designed for a successful transmission. The behavior of the transmission medium that cannot be influenced by the system engineer is depicted by the channel block, residing at the center of the model diagram.

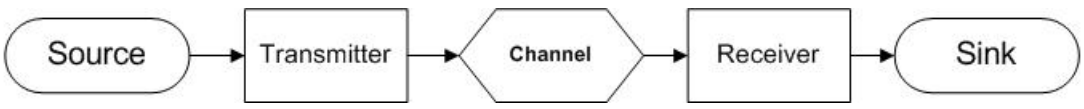

Figure 2.1: Communication system model

The design of a successful communication system requires a good model for the transmission channel. In other words, having a good description of the

communication channel enables better design of the system. So far, experts have worked hard to describe phenomena accompanying different channels, and at the same time to come up with some descriptive and simple mathematical models for further analysis of the system. Actually, there are three channel models that are commonly used in the analysis of a communication system [1]. These models are Additive White Gaussian Noise (AWGN), Linear Time Invariant (LTI) and Linear Time Variant (LTV) channels.

AWGN channel is the simplest channel model that considers only a single channel impairment: noise $n(t)$. The model is depicted in Figure 2.2 and it does not take into account the effect of any fading or distortions. This model is usually used to come up with tractable mathematical models of communication system functionalities so that a better understanding of a system without fading and other distortions is possible. Furthermore, this model is well suited for wired and satellite communication.

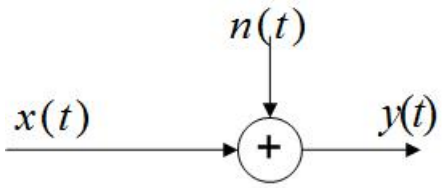

Figure 2.2: AWGN channel model

The second model, LTI channel model, includes deterministic linear distortion in addition to the random AWG noise. Here, the deterministic distortion is modeled by a linear time invariant filter with an impulse response of $c(t)$. This model is usually applied to analyze and design the functionalities of both transmitter and receiver since linearity and time invariability properties of the filter enables usage of good mathematical tools.

Most wireless channels are time variant due to the mobility of the transmitter and receiver and hence the third model called as LTV channel is used. In this model, time varying filter with impulse response $h(\tau, t)$ is used. Here $h(\tau, t)$ is the response of the channel at time t due to an impulse applied at time $t - \tau$ [2]. This model is more complex than LTI channel. As a result, LTI channel model may still be used given that the channel is varying slowly

compared to the time scale of the communication processes analyzed. LTI and LTV channels models are shown in Figure 2.3 and Figure 2.4 respectively.

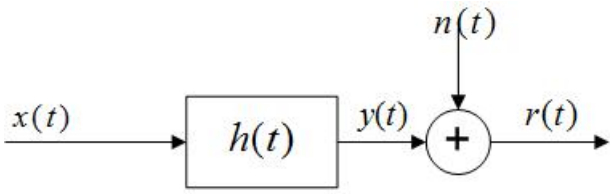

Figure 2.3: LTI channel model

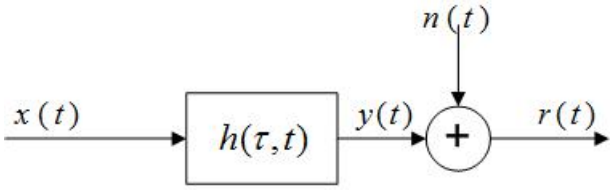

Figure 2.4: LTV channel model

Keeping in mind that wireless channels are in the focus of this thesis, understanding of LTV channels and the overall system model from analytical point of view is important. Therefore, brief and short discussion on signal and system modeling, and LTV channels will be covered in the coming two sections.

2.2 Signal and System Model

Almost all types of wireless transmission are passband communication, where the system signal energy is concentrated in a region close to a given carrier frequency f_0. Thus, the transmitted signal, the channel and the noise that are involved in a given wireless communication system are all passband since out-of-band components are filtered away. From the theory of signals and systems, it is known that the bandpass signal and stochastic processes take the following form:

$$s_p(t) = A(t)\cos(2\pi f_o t + \theta(t)). \tag{2.1}$$

Though wireless communication is bandpass, its baseband equivalent model is usually applied for system analysis and design. This is because bandpass

systems are not as convenient as the baseband system from analysis and simulation perspectives; and furthermore, digital signal processing takes place at baseband. In the baseband equivalent model, the baseband equivalent of each signal or stochastic process $s(t)$ is obtained from its passband equivalent $s_p(t)$ according to the following formulation:

$$\begin{aligned} s_p(t) &= A(t)\cos(2\pi f_o t + \theta(t)) \\ &= A(t)\cos(\theta(t))\cos(2\pi f_o t) - A(t)\sin(\theta(t))\sin(2\pi f_o t) \\ &= s_i(t)\cos(2\pi f_o t) - s_q(t)\sin(2\pi f_o t) \\ &= Re\{s(t)e^{j2\pi f_o t}\} \end{aligned} \tag{2.2}$$

where

$$s_i(t) = A(t)\cos(\theta(t)), \tag{2.3}$$

$$s_q(t) = A(t)\sin(\theta(t)), \tag{2.4}$$

and

$$s(t) = s_i(t) + j s_q(t). \tag{2.5}$$

It is clear that the passband $s_p(t)$ is real valued but its baseband equivalent $s(t)$ is complex valued.

A simple LTI passband system shown in Figure 2.5 can be modeled and analyzed with its baseband equivalent shown in Figure 2.6. Reference [2] has shown that the input-output relationships of the bandpass and its equivalent baseband model are very similar. Here we will briefly present the analysis.

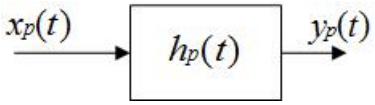

Figure 2.5: Simple passband system

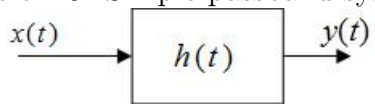

Figure 2.6: Baseband equivalent model

Provided that the Fourier transform of a given signal $s(t)$ is defined as

$$S(f) = \int_{-\infty}^{\infty} s(t)e^{-j2\pi f_o t}dt, \tag{2.6}$$

we have

$$Y_p(f) = H_p(f)X_p(f), \tag{2.7}$$

where $Y_p(f)$, $H_p(f)$ and $X_p(f)$ are the Fourier transforms of $y_p(t)$, $h_p(t)$ and $x_p(t)$, respectively, shown in Figure 2.7.

Obviously, real valued passband signal spectrum $Y_p(f)$ possesses both positive and negative frequency spectrum, denoted by $Y_p^+(f)$ and $Y_p^-(f)$, respectively. The baseband equivalent signal $Y(f)$, which is the Fourier transform of $y(t)$, can be expressed with the positive spectrum $Y_p^+(f)$ as $Y(f) = 2Y_p^+(f + f_o)$. The same formulation is also valid for the other baseband equivalent signals. Therefore,

$$\begin{aligned} Y(f) &= 2Y_p^+(f + f_o) \\ &= 2Y_p(f + f_o)U(f + f_o) \\ &= 2H_p(f + f_o)X_p(f + f_o)U(f + f_o) \\ &= \frac{1}{2}\{2H_p(f + f_o)U(f + f_0)\}\{2X_p(f + f_o)U(f + f_o)\} \\ &= \frac{1}{2}H(f)X(f), \end{aligned} \tag{2.8}$$

where $H(f)$ and $X(f)$ are the Fourier transform of $h(t)$ and $x(t)$, and $U(f)$ is the Fourier transform of the unit step signal $u(t)$, which is defined as

$$u(t) = \begin{cases} 1 & t \geq 0 \\ 0 & t < 0. \end{cases} \tag{2.9}$$

Now the similarity between the passband and its baseband equivalent is clearly seen from equation 2.7 and equation 2.8. Therefore, it is reasonable to analyze a passband system using its baseband equivalent. Furthermore, the system equivalence justification is also described in detail in Appendix 2 of [3].

2.3 Wireless LTV Channels

The basic effects of wireless channel on a transmitted signal are delay, large scale and small scale attenuation, and non-linear dispersion of power in time and frequency. These effects are mainly caused by free space propagation, absorption, wall attenuation and multipath propagation due to reflection, diffraction, and scattering. Furthermore, the wireless medium is characterized by time variation which is unpredictable to the user of the channel. This unpredictability leads to the need of statistical channel model. For these reasons, the channel is modeled as a linear time-varying random filter whose impulse response can be expressed as a set of complex baseband channel gains at a given time t and a given delay τ, $h(\tau, t)$.

Fading is a general term used to give a picture of a wireless channel affected by some type of selectivity. When a channel varies as a function of time, frequency or space in a given window of interest, it is said that the channel possesses selectivity in that window. In contrast, a channel has coherence, which is opposite of selectivity, if it does not change as a function of time, frequency or space over a specified window of interest. Classifying a wireless channel dependency on time, frequency and space as coherent or selective is an essential concept in channel modeling.

A wireless channel shows temporal selectivity which is mostly caused by the motion of either of the transmitter, receiver, scatterer or any combination of them. The motion results in time variation of the phases of the signals of the paths in the multipath propagation. Due to these phase variations as a function of time, the signals interfere constructively or/and destructively in different ways at different time giving variable amplitude at the receiver. It is said that a wireless channel has temporal coherence in a given period of time T_c if the envelope of an unmodulated carrier wave transmitted through the channel is almost static over T_c. The average largest value of T_c is called coherence time, and it measures approximately the time interval over which the channel appears static. A wireless channel shows frequency selectivity due to the time dispersion effects of the multipath propagation. It is also said that a wireless channel has frequency coherence over a given frequency range B_c if the envelope of a transmitted carrier does not change over B_c. The

average largest value of B_c is called coherence bandwidth and is the measure of an approximate range of frequencies over which the channel appears static. Furthermore, a wireless channel has spatial selectivity if the magnitude of a carrier wave change over a spatial displacement of the receiver, and coherence distance D_c is the approximate distance that a wireless receiver can move with the channel appearing to be static. While frequency incoherence is caused by multipaths arriving with different time delays, spatial incoherence is caused by multipaths arriving from different directions in space.

The transmitted signal characteristics affect the selection of an appropriate wireless channel model. Suppose we are transmitting digital information over the channel by modulating a basic pulse with signaling interval of T. If the transmitted signal bandwidth B is greater than the coherence bandwidth of the channel B_c, then the signal is subject to different gains and phase shifts across the band; and therefore, the channel is said to be frequency selective. On the other hand, if the signal bandwidth B is smaller than the coherence bandwidth B_c, the channel is called flat fading or frequency non-selective. In this case all the frequency components in the signal experience the same attenuation and phase shift. The relation between the signaling interval T and channel coherence bandwidth T_c determines whether the channel is slow or fast fading channel. When T is smaller than T_c, the channel attenuation and phase shift are essentially fixed for the duration of at least one signaling interval. When this condition holds, the channel is called slow fading channel. On the contrary, when T is larger than the channel coherence time T_c, the channel is said to be fast fading. Furthermore, if the distance traversed by a receiver is greater than the coherence distance D_c of the channel, it is said that the channel experiences small-scale fading. If the converse is true, the channel experiences large-scale fading.

A wireless channel is often modeled as block fading such that the channel gain is considered constant within a given transmission block while varying independently between different blocks.

2.4 Signal Model Description

In this thesis, the wireless channel is considered to be flat and block fading channel. Flat fading channel is a simple and reasonable model for narrowband systems. In the current OFDM systems, flat fading model is visible within a single OFDM sub-carrier. OFDM modulates low symbol rate data in parallel multiple narrow band sub-carriers. As a result, the multipath delay spread becomes short relatively to the symbol duration. Therefore, the transmitted signal experiences almost the same fading by the channel within the bandwidth of the sub-carrier.

Let us consider Figure 2.4 where the low-pass equivalent $x(t)$ is transmitted over the wireless channel with an impulse response of $h(\tau, t)$. The equivalent low-pass received signal $y(t)$ can be expressed as follows:

$$y(t) = \int_{-\infty}^{\infty} H(f;t)X(f)e^{j2\pi ft}df. \tag{2.10}$$

The $H(f;t)$ and $X(f)$ are the Fourier transform of $h(\tau;t)$ and $x(t)$ respectively. Considering the channel as flat fading implies that $H(f;t)$ is constant in the frequency within the bandwidth occupied by $x(t)$. Therefore, equation 2.10 can be simplified to

$$y(t) = H(0;t)\int_{-\infty}^{\infty} X(f)e^{j2\pi ft}df = H(f_0;t)x(t) = H(0;t)x(t). \tag{2.11}$$

The frequency f_0 can be selected to be any frequency within the bandwidth of the signal $x(t)$. Since the signal is low-pass, zero is taken as the best selection for f_0. Furthermore, the block fading assumption of the channel implies that there is no time variability of the channel in a given block of units. Thus, $H(0;t)$ can be equated with a time-domain complex random variable, let say h_c, for each group. Equation 2.11 is reduced to

$$y(t) = h_c x(t). \tag{2.12}$$

The overall model used throughout this thesis is depicted in Figure 2.7 and

the model can also be described with the following equation:

$$r(t) = h_c x(t) + n(t), \tag{2.13}$$

in which $x(t)$ denotes the transmitted signal and it can be expressed as $x(t) = \sum_{k=-\infty}^{\infty} a_k p(t - kT)$, where a_k denotes the digital transmitted symbol that depends on the modulation technique used by the system, $p(t)$ denotes the pulse shape that is used to transmit the symbols, T denotes the symbol period, h_c is time invariant complex random process that describes the channel, and $n(t)$ is additive white Gaussian noise.

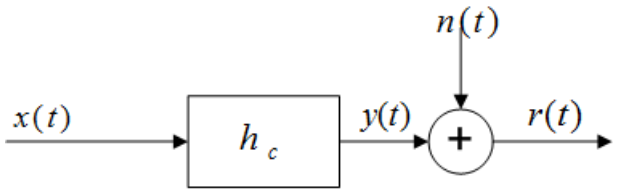

Figure 2.7: Radio link model

In practical cellular systems, interference from neighbouring co-channel transmissions exists at a given target receiver in addition to the desired signal. Therefore, in the presence of interference from M neighbouring transmitters, the above interference free link model is modified as depicted in Figure 2.8. In this case, the signal $r(t)$ is written as

$$r(t) = h_c x(t) + \sum_{m=1}^{M} h_{cm} x_m(t) + n(t) \tag{2.14}$$

where $x(t)$ is the desired transmitted signal, $\{x_m(t) : m = 1, 2, \ldots M\}$ is the set of interference signals, h_c is the channel experienced by the desired signal, $\{h_{cm} : m = 1, 2, \ldots M\}$ is a set of the channel experienced by the M interference signals, and $n(t)$ is the additive white Gaussian noise at the receiver.

Understanding the statistical modeling of the wireless channel is an important step in the analysis and modeling of wireless communication systems. Consequently, statistical fading channel models and related distributions are

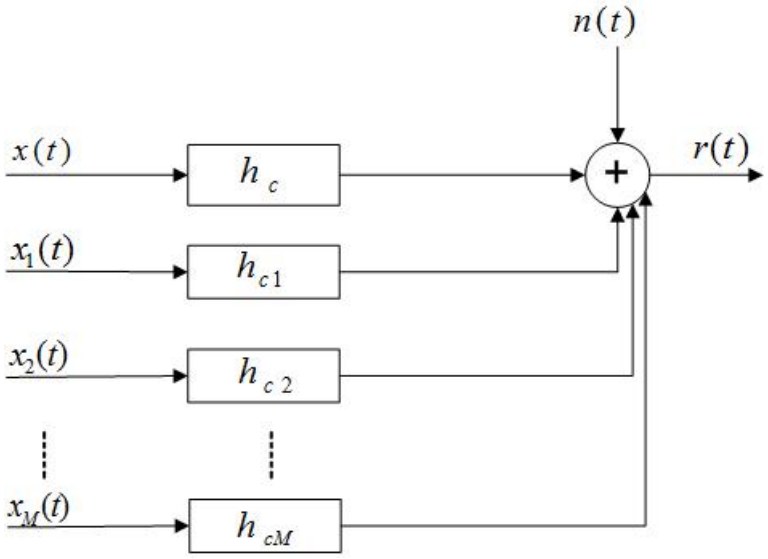

Figure 2.8: Link model in the presence of multiple interfering transmitters

the core part of the discussion in the next chapter.

Chapter 3

Statistical Distributions and Channel Modeling

Probability distribution is an essential tool for a thorough understanding of statistical channel modeling. Therefore, this chapter first covers the required basics of probability theory and then it proceeds to a detailed description of distributions that are used to model fading channels. Finally, with the help of the distribution tools, statistical fading channels modeling is discussed and analyzed in detail.

3.1 Basics in Probability Theory

In probability theory, the set of all possible outcomes of a random trial is called sample space. Random variable is a real-valued function which is defined on the sample space.

The cumulative distribution function (CDF) of a random variable X is a function $F_X(x) : \Re \rightarrow [0, 1]$ defined as follows:

$$F_X(x) = P\{X \leq x\}, \tag{3.1}$$

where $P\{z\}$ is the probability of an event z.

A random variable X is continuous if there is an integrable function $f_X(x)$:

$\Re \rightarrow \Re_+$ such that for all $x \epsilon \Re$

$$F_X(x) = \int_{-\infty}^{x} f_X(w)dw. \tag{3.2}$$

The function $f_X(x)$ is called probability density function.

For a given random variable X, the definitions of the k^{th} raw moment, mean (expected value), variance, moment generating function, and characteristic function are all given below:

$$\begin{aligned}
&\mathrm{E}[X^k] = \int_{-\infty}^{\infty} x^k f_X(x)dx, \qquad \mu_X = \mathrm{E}[x] = \int_{-\infty}^{\infty} x f_X(x)dx,\\
&\mathrm{VAR}[X] = E[(X-\mu_X)^2] = \int_{-\infty}^{\infty} (x-\mu_X)^2 f_X(x)dx,\\
&M_X(s) = \mathrm{E}[e^{sx}] = \int_{-\infty}^{\infty} e^{sx} f_X(x)dx,\\
&\phi_X(w) = \mathrm{E}[e^{jwx}] = \int_{-\infty}^{\infty} e^{jwx} f_X(x)dx.
\end{aligned}$$

MGF and CF are useful tools for statistical analysis. It can be seen from definitions that $\phi_X(w) = M_X(jw)$. If all raw moments of X does not exist, then certainly $M_X(s)$ does not exist but the converse is not true. Furthermore, $\phi_X(w)$ always exists and $\mathrm{E}[X^k] = \frac{d^k M_X(s)}{ds^k}|_{s=0}$.

Suppose that $\{X_j : \quad j = 1, 2, \ldots m\}$ is a set of m random variables. Then their joint statistical behavior is characterized by joint PDF denoted by $f(x_1, x_2, \ldots, x_m)$. These random variables are called independent from one another iff

$$f(x_1, x_2, \ldots, x_m) = f_{X_1}(x_1) f_{X_2}(x_2) \ldots f_{X_m}(x_m), \tag{3.3}$$

and they are said identically distributed if

$$f_{X_1}(x) = f_{X_2}(x) = \ldots = f_{X_m}(x). \tag{3.4}$$

Variables can be both independent and identically distributed (*iid*).

Function of a random variable provides another random variable with its own PDF. Suppose g is an invertible and monotonical function of a single

random variable X such that $Y = g(X)$. Then the PDF of Y in terms of the PDF of X is given by

$$f_Y(y) = |\frac{d}{dy} g^{-1}(y)| f_X(g^{-1}(y)). \tag{3.5}$$

The maximum and minimum of a given set of random variables $\{X_j : j = 1, 2, 3, \ldots m\}$ are also random variables. If X_{max} denotes the maximum and X_{min} denotes the minimum, then the following equations are valid for the two random variables:

$$P\{X_{max} \leq x\} = P\{X_1 \leq x, X_2 \leq x, X_3 \leq x, \ldots, X_m \leq x\}, \tag{3.6}$$

$$P\{X_{min} \geq x\} = P\{X_1 \geq x, X_2 \geq x, X_3 \geq x, \ldots, X_m \geq x\}. \tag{3.7}$$

In digital communication, signal from an information source, communication channel and noise generated at the receiver are usually random and functions of time. At any given time instant, the value of each of them is a random variable. Therefore, they can be characterized by a collection of random variables which is called as random process or stochastic process.

3.2 Distributions for Fading

3.2.1 Gaussian/Normal Distribution

Let X be a random variable that follows Gaussian distribution with parameters μ and σ (usually denoted $X \sim N(\mu, \sigma^2)$). Then its PDF, CDF, MGF, Mean and Variance are given in Table 3.1. In the table, the *error function* is defined

$$f_X(x) = \frac{1}{\sigma\sqrt{2\pi}} e^{-\frac{(x-\mu)^2}{2\sigma^2}}, \qquad F_X(x) = \frac{1}{2}\left[1 + \text{erf}\left(\frac{x-\mu}{\sigma\sqrt{2}}\right)\right].$$
$$\text{E}[x^k] = (-i\sigma\sqrt{2} \cdot \text{sgn}(\mu))^k U\left(\frac{-k}{2}, \frac{1}{2}, \frac{-\mu^2}{2\sigma^2}\right).$$
$$M_X(s) = e^{\mu s + \frac{1}{2}\sigma^2 s^2}, \qquad \text{E}[X] = \mu, \qquad \text{VAR}[X] = \sigma^2.$$

Table 3.1: Characterization of Gaussian distribution

by the relation

$$\text{erf}(z) = \frac{2}{\sqrt{\pi}} \int_0^z e^{-t^2} dt, \qquad [4, \text{ eqn } 7.1.1] \tag{3.8}$$

and the *confluent hypergeometric function* $U(\cdot, \cdot, \cdot)$ is defined in [4, eqn 13.1.3]. In the real axis, $\text{erf}(-\infty) = -1, \text{erf}(0) = 0, \text{erf}(\infty) = 1$ and $\text{erf}(-x) = -\text{erf}(x)$.

The general formula for the raw moments of X is complicated due to the confluent hypergeometric function, but the moments can be computed easily for small values of k using the formula $\text{E}[X^k] = \frac{d^k M(s)}{ds^k}[0]$. Furthermore, the central moments are

$$\text{E}[(x-\mu)^n] = \begin{cases} \frac{(2k)!\sigma^{2k}}{2^k k!}, & \text{for } n = 2k, \\ 0, & \text{for } n = 2k+1. \end{cases} \tag{3.9}$$

The distribution fulfils the following properties:

- If $X \sim N(\mu, \sigma^2)$, and $a, b \in \Re$, then $aX + b \sim N(a\mu + b, a^2\sigma^2)$.
- If $\{X_i, i = 1, 2, \ldots, n\}$ are independent variables such that $X_i \sim N(\mu_i, \sigma_i^2)$, then $\sum_{i=1}^n X_i \sim N(\sum_{i=1}^n \mu_i, \sum_{i=1}^n \sigma_i^2)$.

Gaussian distribution has nearly a 300 years history since it was discovered by de Moivre in 1733, and a large number of related literatures have been written in this period. This distribution is used as a model for many complex phenomena in various fields of science. Majority of the scientific community agree that the justification for the success of this distribution is Central Limit Theorem, which will be stated below. Reference [5] describes other additional key characteristics of Gaussian distribution that contribute for its wide usage.

Central Limit Theorem [6]: Let $\{X_i : \ i = 1, 2, \ldots, N\}$ be statistically independent random variables with $\text{E}[X_i] = \mu_i$ and $\text{VAR}[X_i] = \sigma_i^2$. Then, the random variable

$$Y = \lim_{N\to\infty} \frac{1}{\sqrt{N}} \sum_{n=1}^{N} (X_i - \mu_i) \tag{3.10}$$

is asymptotically normally distributed with the expected value $\text{E}[Y] = 0$ and the variance $\text{VAR}[Y] = \sigma_Y^2 = \lim_{N\to\infty} \frac{1}{N} \sum_{n=1}^N \sigma_i^2$.

In general the sum of a large number of independent factors is usually considered as normally distributed random variable. Noise in communication system, for instance, is often considered as Gaussian distributed variable.

3.2.2 Central and Noncentral Chi-square Distribution

Central Chi-square Distribution

Let $\{X_i : i = 1, 2, \ldots, n\}$ be *iid* variables such that $X_i \sim N(0, \sigma^2)$, $\forall i$. Then $X = \sum_{i=1}^{n} X_i^2$ is defined as a *chi-square* random variable with n degrees of freedom. Its description is given in Table 3.2. In the description we employ

$$f_X(x) = \begin{cases} \frac{1}{2^{\frac{n}{2}}\Gamma(\frac{n}{2})\sigma^n} x^{\frac{n}{2}-1} e^{-\frac{x}{2\sigma^2}}, & x > 0, \\ 0, & x \leq 0. \end{cases}$$

$$\text{For } n = 2m, \quad F_X(x) = \begin{cases} 1 - e^{\frac{-x}{2\sigma^2}} \sum_{j=1}^{m-1} \frac{1}{j!} (\frac{x}{2\sigma^2})^j, & x > 0, \\ 0, & x \leq 0. \end{cases}$$

$$\mathrm{E}[X^k] = \begin{cases} (2\sigma^2)^k \frac{\Gamma(m+k)}{(m-1)!}, & \text{for } n = 2m, \\ (2\sigma^2)^k \frac{\Gamma(m+k+\frac{1}{2})}{\Gamma(m+\frac{1}{2})}, & \text{for } n = 2m+1. \end{cases}$$

$$M_X(s) = \left(\frac{1}{1-2\sigma^2 s}\right)^{\frac{n}{2}}, \qquad \mathrm{E}[X] = n\sigma^2, \qquad \mathrm{VAR}[X] = 2n\sigma^4.$$

Table 3.2: Characterization of central chi−square distribution

the *Gamma function*

$$\Gamma(z) = \int_0^\infty t^{z-1} e^{-t} dt. \qquad [4, \text{eqn } 6.1.1] \tag{3.11}$$

Gamma function possesses poles at $0, -1, -2, \ldots$, and it admits the following identities: $\Gamma(1) = 1$, $\Gamma(\frac{1}{2}) = \sqrt{\pi}$, and $\Gamma(x+1) = x\Gamma(x)$. As can be seen from Table 3.2, $F_X(x)$ is given only for $n = 2m$. This is due to the fact that there is no closed-form expression for $n = 2m + 1$.

Chi-square random variable is a special case of two parameter gamma random variable with a shape parameter $\frac{n}{2}$ and a scale parameter $2\sigma^2$ [7]. In

addition, if $n = 2$, then it is equal to exponential distribution with mean $2\sigma^2$.

Noncentral Chi-square Distribution

Let $\{X_i : i = 1, 2, \ldots, n\}$ be independent variables with the same variance but different means such that $X_i \sim N(\mu_i, \sigma^2)$. Then $X = \sum_{i=1}^{n} X_i^2$ is defined as a *noncentral chi-square* random variable with n degrees of freedom. In the following we use notation $a = \sqrt{\sum_{i=1}^{n} \mu_i^2}$. Table 3.3 gives characterization of noncentral chi-square distribution.

$$f_X(x) = \begin{cases} \frac{1}{2\sigma^2}(\frac{x}{a^2})^{\frac{n-2}{4}} e^{-\frac{a^2+x}{2\sigma^2}} \mathbf{I}_{\frac{n}{2}-1}(\frac{a}{\sigma^2}\sqrt{x}), & x > 0, \\ 0, & x \le 0. \end{cases}$$

$$\text{For } n = 2m, \quad F_X(x) = \begin{cases} 1 - Q_m(\frac{a}{\sigma}, \frac{\sqrt{x}}{\sigma}), & x > 0, \\ 0, & x \le 0. \end{cases}$$

$$\mathrm{E}[X^k] = \begin{cases} (2\sigma^2)^k e^{-\frac{a^2}{2\sigma^2}} \frac{(m+k-1)!}{(m-1)!} M(m+k, m, \frac{a^2}{2\sigma^2}), & \text{for } n = 2m, \\ (2\sigma^2)^k e^{-\frac{a^2}{2\sigma^2}} \frac{\Gamma(m+k+\frac{1}{2})}{\Gamma(m+\frac{1}{2})} M(m+k+\frac{1}{2}, m+\frac{1}{2}, \frac{a^2}{2\sigma^2}), & \text{for } n = 2m+1. \end{cases}$$

$$M_X(s) = \left(\frac{1}{1-2\sigma^2 s}\right)^{\frac{n}{2}} e^{\frac{a^2 s}{1-2\sigma^2 s}}, \qquad \mathrm{E}[X] = n\sigma^2 + a^2, \quad \mathrm{VAR}[X] = 2n\sigma^4 + 4\sigma^2 a^2$$

Table 3.3: Characterization of noncentral chi-square distribution

In Table 3.3 we used the *Modified Bessel function of the first kind and order* v, the *generalized Marcum Q function*, and the *confluent hypergeometric function*. Their definitions are given as follows:

$$\mathbf{I}_v(z) = (\frac{1}{2}z)^v \sum_{k=0}^{\infty} \frac{(\frac{1}{4}z^2)^k}{k!\Gamma(v+k+1)}, \qquad [4, \text{eqn } 9.6.10] \tag{3.12}$$

$$Q_m(c, d) = \int_d^{\infty} x(\frac{x}{c})^{m-1} e^{-\frac{x^2+c^2}{2}} \mathbf{I}_{m-1}(cx)dx, \qquad [8] \tag{3.13}$$

$$M(a, b, z) = \frac{\Gamma(b)}{\Gamma(b-a) - \Gamma(a)} \int_0^1 e^{zt} t^{a-1}(1-t)^{b-a-1} dt. \; [4, \text{eqn } 13.2.1] \tag{3.14}$$

See (3.11) for $\Gamma(\cdot)$ and (3.12) for $I_v(z)$.

Closed-form expression of the CDF for $n = 2m + 1$ does not exist.

Some authors define both central and noncentral chi-square distributions in a slightly different way than we did. The difference occurs because some authors consider the variance of the normally distributed variables to be equal to unity. Let X' be central chi-square variable according to the unit variance definition and let X be central chi-square variable according to the definition which was discussed. It can be shown that X' is related with X as

$$X' = \frac{1}{\sigma^2} X. \tag{3.15}$$

The same relation is valid for the noncentral chi-square definitions. Therefore, a simple mapping of functions or values according to one definition to the corresponding functions or values according to other definition is possible.

Chi-square distributions are used in the analysis of wireless systems. For instance, the randomly time-varying multiple-input multiple-output (MIMO) channel is characterized by $N_R \times N_T$ channel matrix, H, of elements h_{ij}, where h_{ij} is the equivalent lowpass channel impulse response between the j^{th} transmit antenna and the i^{th} receiver antenna. The performance of MIMO systems is determined by a squared Frobenius norm parameter $||H||_F^2 = \sqrt{\sum_{i=1}^{N_R} \sum_{j=1}^{N_T} |h_{ij}|^2}$. For the commonly used fading channel model, $\{h_{ij}\}$ is assumed as *iid* complex-valued zero mean Gaussian. In this case, $||H||_F^2$ is a chi-squared variable with $2N_R N_T$ degrees of freedom. Therefore chi-square distribution is a useful tool in the analysis of the performance of MIMO systems.

3.2.3 Rayleigh Distribution

Let $\{X_i : i = 1, 2, \ldots, n\}$ be *iid* zero mean Gaussian random variables such that $X_i \sim N(0, \sigma^2)$, $\forall i$. Then $X = \sqrt{\sum_{i=1}^{n} X_i^2}$ is defined as a *generalized Rayleigh* random variable. When $n = 2$ in the equation, we get the *Rayleigh distribution*. Its PDF, CDF, MGF, raw moments, mean and variance are given in Table 3.4. For special functions $M(\cdot, \cdot, \cdot)$ and $\Gamma(\cdot)$, see (3.14) and (3.11).

Rayleigh distribution is used to model small-scale fading in wireless communication channel when the channel is characterized by a large number of scatterers and there is no dominant path or a line of sight connection. For instance, urban areas in mobile communication mostly have this kind of channel.

$$f_X(x) = \begin{cases} \frac{x}{\sigma^2} e^{-\frac{x^2}{2\sigma^2}}, & x > 0, \\ 0, & x \leq 0, \end{cases} \qquad F_X(x) = \begin{cases} 1 - e^{\frac{-x^2}{2\sigma^2}}, & x > 0 \\ 0, & x \leq 0. \end{cases}$$

$$\mathrm{E}[X^k] = (2\sigma^2)^{\frac{k}{2}} \Gamma\left(\frac{k}{2} + 1\right), \qquad M_X(s) = M\left(1, \frac{1}{2}, \frac{1}{2}\sigma^2 s^2\right) + \sqrt{\frac{\pi}{2}} \sigma s e^{\frac{\sigma^2 s^2}{2}}.$$

$$\mathrm{E}[X] = \sigma\sqrt{\frac{\pi}{2}}, \qquad \mathrm{VAR}[X] = \left(\frac{4-\pi}{2}\right)\sigma^2.$$

Table 3.4: Characterization of Rayleigh distribution

According to central limit theorem of subsection 3.2.1, the baseband equivalent impulse response of a channel with a large number of scatterers can be modeled by a zero mean complex Gaussian process. Therefore, the envelope of the channel impulse response is the square root of the sum of the squares of two zero mean Gaussian random processes. By definition, this process is Rayleigh. Furthermore, based on extensive measurements of the envelope of the received signal at the receiver, [9], [10] and [11] suggested Rayleigh process as a suitable model in urban and suburban areas.

3.2.4 Rician Distribution

Let $\{X_i : i = 1, 2, \ldots, n\}$ be independent Gaussian random variables with same variance but different mean such that $X_i \sim N(\mu_i, \sigma^2)$, $\forall\ i$. Then $X = \sqrt{\sum_{i=1}^{n} X_i^2}$ is defined as a *generalized Rician* random variable. When $n = 2$ in the equation, we get the *Rician distribution*. In what follows, we denote $a = \sqrt{\sum_{i=1}^{n} \mu_i^2}$. The Rician distribution descriptions are given in Table 3.5. For the special functions $Q_m(c, d)$ and $M(a, b, z)$ in Table 3.5, see (3.13) and (3.14). Rician distribution does not have a closed form MGF.

Rice process is chosen as a suitable model of wireless channel when there is a dominant path or line of sight connection between the transmitter and receiver. Rural areas in mobile communication, for instance, usually possess this kind of channel. In the presence of a dominant or line-of-sight component, we get the sum of the scattered components and line of sight components at the receiver. According to central limit theorem of subsection (3.2.1), the baseband equivalent of the sum is a complex Gaussian process. Furthermore,

$$f_X(x) = \begin{cases} \frac{x}{\sigma^2} e^{-\frac{x^2+a^2}{2\sigma^2}} I_0(\frac{ah}{\sigma^2}), & x > 0, \\ 0, & x \leq 0, \end{cases} \quad F_X(x) = \begin{cases} 1 - Q_1\left(\frac{a}{\sigma}, \frac{x}{\sigma}\right), & x > 0 \\ 0, & x \leq 0. \end{cases}$$

$$\mathrm{E}[X^k] = (2\sigma^2)^{\frac{k}{2}} e^{-\frac{a^2}{2\sigma^2}} \Gamma\left(1 + \frac{k}{2}\right) M\left(1 + \frac{k}{2}, 1; \frac{a^2}{2\sigma^2}\right), \qquad \mathrm{E}[X^2] = 2\sigma^2 + a^2.$$

$$\mathrm{E}[X] = \sigma\sqrt{\frac{\pi}{2}} M\left(-\frac{1}{2}, 1; -\frac{a^2}{2\sigma^2}\right), \qquad \mathrm{VAR}[X] = \mathrm{E}[X^2] - (\mathrm{E}[X])^2.$$

Table 3.5: Characterization of Rician distribution

due to the dominant path, the mean of the real part is different from zero. So the envelope of the impulse response is a Rice process. The scenario is similar with a sinusoidal wave plus random noise which has been treated by Rice [12]. In addition, the analysis based on experimental data in [13] shows that Rician distribution is more accurate than Rayleigh, Nakagami and Weibull distributions in modeling the signal statistics in rural areas. Nakagami and Weibull distribution will be discussed in the subsections (3.2.6) and (3.2.7), respectively.

3.2.5 Lognormal Distribution

Let X be a normally distributed random variable such that $X \sim N(\mu_X, \sigma_X^2)$. Then the variable

$$R = 10^{\frac{X}{10}} \tag{3.16}$$

is a *lognormally distributed* random variable (we denote $R \sim$ Log-N(μ_i, σ_i^2)). Lognormal distribution is characterized by Table 3.6. The constant ξ in Table 3.6 denotes $10/\ln 10$.

The characteristic function of R is not obtainable in closed form but can be approximated by a Gauss-Hermite expansion:

$$\phi_R(w) \cong \frac{1}{\sqrt{\pi}} \sum_{n=1}^{N_p} H_{x_n} \exp\left(\frac{\sqrt{2}\sigma_X x_n + \mu_X}{10} jw\right), \tag{3.17}$$

where x_n are the zeros and H_{x_n} are the weight factors of the N_p-order Hermite

$$f_R(r) = \begin{cases} \frac{\xi}{\sigma_X\sqrt{2\pi}r}\exp\left(-\frac{(10\log_{10}r-\mu_X)^2}{2\sigma_X^2}\right), & r>0, \\ 0, & r\le 0. \end{cases}$$

$$F_R(r) = \begin{cases} 1-Q\left(\frac{10\log_{10}r-\mu_X}{\sigma_X}\right), & r>0, \\ 0, & r\le 0, \end{cases} \qquad \mathrm{E}[R^k] = \exp\left(\frac{k}{\xi}\mu_X + \frac{1}{2}(\frac{k}{\xi})^2\sigma_X^2\right).$$

$$\mathrm{E}[R] = \exp\left(\frac{\mu_X}{\xi} + \frac{1}{2}(\frac{\sigma_X}{\xi})^2\right), \quad \mathrm{VAR}[X] = \mathrm{E}[R^2] - (\mathrm{E}[R])^2.$$

Table 3.6: Characterization of lognormal distribution

polynomial [14]. If $\{R_i : i = 1, 2, \ldots, n\}$ is a set of n independent lognormally distributed variables such that $R_i \sim \text{Log-N}(\mu_i, \sigma_i^2)$, $\forall i$, then

$$\prod_{i=1}^{n} R_i \sim \text{Log-N}\left(\sum_{i=1}^{n}\mu_i, \sum_{i=1}^{n}\sigma_i^2\right). \tag{3.18}$$

Lognormal distribution is used to model large-scale fading which is caused by shadowing. Though measurements show that lognormal distribution is a suitable model for shadow fading [11], there is no satisfactory justification of the model. Thus, lognormal model of the shadow fading is just an acceptable practical tool for modeling shadow fading without a good explanation from the propagation point of view. The product of a large number of positive independent random variables might also be modeled by lognormal distribution.

3.2.6 Nakagami Distribution

A Nakagami-distributed random variable X is characterized by Table 3.7. In Table 3.7, the following notations are used: $\Omega = \mathrm{E}[X^2]$ and $m = \frac{\Omega^2}{E[(X^2-\Omega)^2]}$. Parameter m is usually called *fading figure* and the distribution is defined only for $m \ge \frac{1}{2}$. The *incomplete gamma function* needed in Table 3.7 is defined as

$$\gamma(u, x) = \int_0^x t^{u-1}e^{-t}dt. \tag{3.19}$$

Nakagami distribution does not have a general closed form MGF.

Nakagami random variable becomes a Rayleigh random variable when $m =$

$$f_X(x) = \begin{cases} \frac{2}{\Gamma(m)}\left(\frac{m}{\Omega}\right)^m x^{2m-1}\exp\left(-\frac{mx^2}{\Omega}\right), & x > 0, \\ 0, & x \leq 0. \end{cases}$$

$$F_X(x) = \begin{cases} \frac{\gamma(m,\frac{m}{\Omega}x^2)}{\Gamma(m)}, & x > 0, \\ 0, & x \leq 0, \end{cases} \qquad \mathrm{E}[x^k] = \frac{\Gamma\left(m+\frac{k}{2}\right)}{\Gamma(m)}\left(\frac{\Omega}{m}\right)^{\frac{k}{2}}.$$

$$\mathrm{E}[X] = \frac{\Gamma(m+\frac{1}{2})}{\Gamma(m)}\left(\frac{\Omega}{m}\right)^{\frac{1}{2}}, \qquad \mathrm{VAR}[X] = \Omega\left(1 - \frac{1}{m}\left(\frac{\Gamma(m+\frac{1}{2})}{\Gamma(m)}\right)^2\right).$$

Table 3.7: Characterization of Nakagami distribution

1. Furthermore, Nakagami PDF possesses larger tails than Rayleigh PDF when $\frac{1}{2} \leq m \leq 1$ but the converse is true when $m > 1$.

Though Nakagami distribution is initially proposed as empirical model for short wave ionospheric propagation, nowadays it is used to model small-scale fading as that of Rayleigh, Rice and Weibull distribution. As it is a two parameter distribution, it provides more flexible and accurate adaptation to a probability density functions which follow from experimental measurement results. Consequently, it can describe different fading environments. Because of this feature, the distribution is used widely in performance analysis these days. Experimental results show that this distribution is the best model of fading in certain special conditions. For example, it is suggested by [15] as the best fit for the distribution of the signals received in urban radio multipath channels.

Nakagami distribution is also used to describe the amplitude of received k branch Rayleigh fading signal after maximum ratio diversity combining. In this case the shape factor m of the distribution is equal to k.

3.2.7 Weibull Distribution

Let X be a random variable that follows a *2-parameter Weibull Distribution* with a scale parameter $\alpha > 0$ and a shape parameter $\beta > 0$. Then, it is characterized by Table 3.8, see (3.11) for $\Gamma(z)$.

Though there is no general closed-form solution found for the MGF, it is given in power series form in Table 3.8 since all the raw moments are known.

$$f_X(x) = \begin{cases} \frac{\beta}{\alpha}(\frac{x}{\alpha})^{\beta-1}e^{-(\frac{x}{\alpha})^{\beta}}, & x > 0, \\ 0, & x \leq 0, \end{cases} \qquad F_X(x) = \begin{cases} 1 - e^{-(\frac{x}{\alpha})^{\beta}}, & x > 0, \\ 0, & x \leq 0. \end{cases}$$

$$M_X(s) = \sum_{n=0}^{\infty} \frac{s^n \alpha^n}{n!} \Gamma\left(1 + \frac{n}{\beta}\right), \qquad \mathrm{E}[X^k] = \alpha^k \Gamma\left(1 + \frac{k}{\beta}\right).$$

$$\mathrm{E}[X] = \alpha\Gamma\left(1 + \frac{1}{\beta}\right), \qquad \mathrm{VAR}[X] = \alpha^2\left[\Gamma\left(1 + \frac{2}{\beta}\right) - \Gamma^2\left(1 + \frac{1}{\beta}\right)\right].$$

Table 3.8: Characterization of Weibull distribution

Moreover, it has also other closed-form expressions when the shape parameter β is integer or rational. The expressions are derived and given in [16], [17] and [18]. When $\beta = 1$, a Weibull PDF reduces to the exponential PDF, and when $\beta = 2$, it reduces to the Rayleigh PDF.

Weibull distribution is another mathematical model for small-scale fading in wireless communication. Empirical studies have shown that Weibull distribution is an effective model of both indoor and outdoor propagation [19, 20]. Furthermore, reference [21] describes Weibull Distribution as a less complex and accurate description for the outdoor multipath fading channel than some of the other existing models.

3.3 Statistical Channel Modeling

Let us start by referring to the link level signal model which we described in the first chapter with the help of Figure 2.7. We recall equation (2.13) as

$$r(t) = h_c x(t) + n(t). \tag{3.20}$$

The transmitted signal $x(t)$ is multiplied by the complex channel h_c and then AWG noise with a one-side power spectral density N_o is added at the receiver to give $r(t)$.

The fading channel is usually modeled with Rayleigh, Rician, Nakagami, Weibull, or/and lognormal distribution depending on the nature of the radio propagation environment. The aforementioned distributions and their role to model small-scale or large-scale fading were discussed in the previous section.

If E_s is the signal energy per transmitted symbol, then the instantaneous SNR at the receiver which we denote by γ is given as

$$\gamma = h^2 \frac{E_s}{N_o}, \tag{3.21}$$

where $h = |h_c|$. Note that h is the amplitude of the complex channel h_c and we will use the notations throughout the thesis accordingly. Then the expected SNR, denoted by $\bar{\gamma}$, is

$$\bar{\gamma} = \mathrm{E}[\gamma] = \mathrm{E}\left[h^2 \frac{E_s}{N_o}\right] = \frac{E_s}{N_o}\mathrm{E}[h^2]. \tag{3.22}$$

Thus,

$$\gamma = \frac{\bar{\gamma}}{\mathrm{E}[h^2]} h^2. \tag{3.23}$$

Notice that γ is a function of the fading channel random variable h. The PDF of h can be obtained from the previous section according to the fading channel model chosen. Then, the PDF of γ can be computed from the PDF of h based on Equation (3.5).

$$\begin{aligned} f_\gamma(\gamma) = & \left| \tfrac{d}{d\gamma} \sqrt{\tfrac{\mathrm{E}[h^2]}{\bar{\gamma}}\gamma} \right| f_h\left(\sqrt{\tfrac{\mathrm{E}[h^2]}{\bar{\gamma}}\gamma}\right) \\ = & \tfrac{1}{2}\sqrt{\tfrac{\mathrm{E}[h^2]}{\bar{\gamma}\gamma}} f_h\left(\sqrt{\tfrac{\mathrm{E}[h^2]}{\bar{\gamma}}\gamma}\right) \end{aligned} \tag{3.24}$$

Rayleigh Fading Channel

In Rayleigh fading channel model, h is considered to be Rayleigh random variable. Therefore, using the mean and variance expressions of Table 3.4,

$$\mathrm{E}[h^2] = \mathrm{VAR}[h] + (\mathrm{E}[h])^2 = \left(\frac{4-\pi}{2}\right)\sigma^2 + \left(\sigma\sqrt{\frac{\pi}{2}}\right)^2 = 2\sigma^2. \tag{3.25}$$

Then using (3.25) and the PDF expression in Table 3.4, (3.24) reduces into

$$f_\gamma(\gamma) = \frac{1}{\bar{\gamma}} e^{-\frac{\gamma}{\bar{\gamma}}}, \qquad \gamma > 0. \tag{3.26}$$

Notice from (3.26) that γ is an exponential random variable with a scale

parameter $\bar{\gamma}$. Therefore,

$$F_\gamma(\gamma) = \int_{-\infty}^{\gamma} f_\gamma(w)dw = 1 - \exp\left(-\frac{\gamma}{\bar{\gamma}}\right), \qquad \gamma > 0, \tag{3.27}$$

$$M_\gamma(s) = \int_{-\infty}^{\infty} e^{s\gamma} f_\gamma(\gamma)d\gamma = \frac{1}{1-\bar{\gamma}s}, \quad \text{for } s < 0. \tag{3.28}$$

It can also be shown that γ is a central chi-square random variable with two degrees of freedom and parameter $\sigma = \sqrt{\frac{\bar{\gamma}}{2}}$.

Rician Fading Channel

In this model, h is considered to be Rician random variable. Therefore, from Table 3.5, we get that

$$\mathrm{E}[h^2] = 2\sigma^2 + a^2. \tag{3.29}$$

In Rician fading channel, there is a parameter called Rician *K-factor* which is defined as

$$K = \frac{a^2}{2\sigma^2}. \tag{3.30}$$

Then $\mathrm{E}[h^2]$ can also be expressed in terms of K as

$$\mathrm{E}[h^2] = 2\sigma^2 + a^2 = 2\sigma^2\left(1 + \frac{a^2}{2\sigma^2}\right) = 2\sigma^2(1+K). \tag{3.31}$$

Using the PDF expression in Table 3.5 and (3.31), Equation (3.24) is simplified into

$$f_\gamma(\gamma) = \frac{(1+K)e^{-K}}{\bar{\gamma}} \exp\left(-\frac{(1+K)\gamma}{\bar{\gamma}}\right) I_0\left(\sqrt{\frac{4K(1+K)\gamma}{\bar{\gamma}}}\right), \ \gamma > 0. \tag{3.32}$$

Refer (3.12) for $I_0(z)$. It can be seen from (3.32) that γ is non-central chi-square random variable with parameters $a = \sqrt{\frac{K\bar{\gamma}}{K+1}}$ and $\sigma = \sqrt{\frac{\bar{\gamma}}{2(K+1)}}$. Therefore, using CDF and MGF expressions of non-central chi-square variable which

are given in Table 3.3, we obtain

$$F_\gamma(\gamma) = 1 - Q_m\left(\sqrt{2K}, \sqrt{\frac{2(K+1)\gamma}{\bar{\gamma}}}\right), \gamma > 0, \tag{3.33}$$

$$M_\gamma(s) = \frac{K+1}{K+1-\bar{\gamma}s} \exp\left(\frac{K\bar{\gamma}s}{K+1-\bar{\gamma}s}\right). \tag{3.34}$$

See (3.13) for $Q_m(\cdot)$.

Nakagami Fading Channel

In Nakagami fading channel model, the amplitude of the channel impulse response is considered to be Nakagami random variable. Thus, from the notation used in Table 3.7, we get

$$\mathrm{E}[h^2] = \Omega. \tag{3.35}$$

Then substituting the PDF in Table 3.7 into (3.24), the PDF of γ becomes

$$f_\gamma(\gamma) = \frac{m^m}{\Gamma(m)\bar{\gamma}^m}\gamma^{m-1}e^{-\frac{m\gamma}{\bar{\gamma}}}, \qquad \gamma > 0, \tag{3.36}$$

We can show from (3.36) that γ is gamma-distributed random variable with shape parameter m and scale parameter $\frac{\bar{\gamma}}{m}$. Consequently,

$$F_\gamma(\gamma) = \frac{\Gamma(m, \frac{m\gamma}{\bar{\gamma}})}{\Gamma(m)}, \qquad \gamma > 0, \tag{3.37}$$

$$M_\gamma(s) = \left(1 - \frac{\bar{\gamma}}{m}s\right)^{-m}. \tag{3.38}$$

Weibull Fading Channel

Here h is a Weibull random variable. Therefore, from Table 3.8, we get that

$$\mathrm{E}[h^2] = \alpha^2\Gamma\left(1 + \frac{2}{\beta}\right). \tag{3.39}$$

Substituting (3.39) and PDF of h from Table 3.8 in (3.24) gives

$$f_\gamma(\gamma) = \frac{\beta}{2b\bar{\gamma}}\left(\frac{\gamma}{b\bar{\gamma}}\right)^{\frac{\beta}{2}-1} e^{-(\frac{\gamma}{b\bar{\gamma}})^{\frac{\beta}{2}}}, \qquad \gamma > 0, \tag{3.40}$$

where $b = 1/\Gamma\left(1+\frac{2}{\beta}\right)$. Refer (3.11) for $\Gamma(\cdot)$.

Notice from 3.40 that γ is also a Weibull random variable with a shape parameter equal to $\frac{\beta}{2}$ and scale parameter equal to $b\bar{\gamma}$. Therefore, using CDF and MGF in Table 3.8,

$$F_\gamma(\gamma) = 1 - \exp\left[-\left(\frac{\gamma}{b\bar{\gamma}}\right)^{\frac{\beta}{2}}\right], \qquad \gamma > 0, \tag{3.41}$$

$$M_\gamma(s) = \sum_0^\infty \frac{(b\bar{\gamma})^n s^n}{n!}\Gamma\left(1+\frac{2n}{\beta}\right). \tag{3.42}$$

Lognormal Fading Channel

Modeling only large-scale fading due to shadowing is important for the analysis of communication system performance if the receiver has the ability to average out or eliminate the effect of small-scale fading. In this situation, the SNR is directly modeled with lognormal distribution. Thus,

$$f_\gamma(\gamma) = \frac{\xi}{\sigma_X\sqrt{2\pi}\gamma}\exp\left(-\frac{(10\log_{10}\gamma - \mu_X)^2}{2\sigma_X^2}\right), \qquad \gamma > 0, \tag{3.43}$$

where $\xi = \frac{10}{\ln(10)}$.

Composite Fading Channel

Some environments comprise small-scale fading superimposed on the lognormal large-scale fading. In this kind of environment, the receiver plays with the instantaneous signal corrupted by the composite fading due to both multipath and shadowing. Therefore, the channel is modeled with composite fading channel. Reference [22] discusses the widely accepted Nakagami-lognormal fading channel model. The composite gamma/lognormal PDF of the SNR is given as follows:

$$f_\gamma(\gamma) = \int_0^\infty \frac{m^m\gamma^{m-1}}{w^m\Gamma(m)}e^{-\frac{m\gamma}{w}}\frac{\xi}{\sqrt{2\pi}\sigma_X w}\exp\left(-\frac{(10\log_{10}w - \mu_X)^2}{2\sigma_X^2}\right)dw. \tag{3.44}$$

In the analysis, the average of the Nakagami-distributed SNR follows lognormal distribution. The integral cannot be calculated in closed-form.

Rayleigh-lognormal distribution used for modeling Rayleigh-lognormal environment has also a complicated integral. Thus, this distribution is usually approximated by K-distribution [23]. The Weibull-lognormal environment characterization is also discussed in [24].

Chapter 4

Link-level Performance Measures in Fading Channels

In this chapter, some widely used radio link performance measures in fading channels are presented. The co-channel interference from neighbouring transmissions is not considered. First, we will summarize expressions for average bit error probability (BEP) with the binary phase shift keying (BPSK) modulation scheme in Rayleigh, Rician, Nakagami, and Weibull fading channels. Then computations and resultant expressions of outage probability/outage capacity and average capacity will be presented for the aforementioned channel models.

4.1 Average BEP of BPSK

Bit error probability is one of the key performance measures in wireless communication and it is defined as the error probability in transmission of a single bit. Average BEP calculation of a wireless communication system is dependent on the modulation scheme and channel model which are used by the system.

In what follows, average BEP for Rayleigh, Rician, Nakagami, and Weibull fading channel models with BPSK modulation scheme are calculated. The average BEP computation for the general quadrature amplitude modulation can be easily managed if the computation for BPSK is understood well [25, 26].

With Binary Phase Shift Keying (BPSK), the BEP in AWGN channel, de-

noted by P_b, is obtained as

$$P_b = Q\left(\sqrt{2\gamma}\right), \qquad [2, \text{eqn 4.3-13}][27] \tag{4.1}$$

where the variable γ denotes symbol SNR. Note also that symbol SNR is the same with bit SNR in case of BPSK modulation scheme. The Gaussian Q function is defined as

$$Q(x) = \frac{1}{\sqrt{2\pi}} \int_x^\infty e^{-\frac{t^2}{2}} dt. \qquad [2, \text{eqn 2.3-10}] \tag{4.2}$$

In fading channels where γ is corrupted by the random fading channel, (4.1) can be taken as the instantaneous BEP expression and the average BEP, which we denote by $\bar{P}_b$, is calculated by integrating it over SNR distribution:

$$\bar{P}_b = \int_0^\infty P_b f_\gamma(\gamma) d\gamma = \int_0^\infty Q\left(\sqrt{2\gamma}\right) f_\gamma(\gamma) d\gamma, \tag{4.3}$$

where $f_\gamma(\gamma)$ is the PDF of the SNR. Various PDF expressions has been computed in the previous chapter for different fading channel models.

Before we start analyzing (4.3) for fading channel models, let us first make the equation suitable for integration by substituting $Q(\sqrt{2\gamma})$ with an alternative expression. Craig has developed the following alternative expression for $Q(x)$ of (4.2) in [28]:

$$Q(x) = \frac{1}{\pi} \int_0^{\frac{\pi}{2}} \exp\left(-\frac{x^2}{2\sin^2\theta}\right) d\theta, \quad \text{for } x \geq 0. \tag{4.4}$$

After using this alternating expression and MGF definition, given in section 3.1 of Chapter 3, equation (4.3) can be reduced into form

$$\bar{P}_b = \frac{1}{\pi} \int_0^{\frac{\pi}{2}} M_\gamma\left(-\frac{1}{\sin^2\theta}\right) d\theta. \tag{4.5}$$

Rayleigh Fading Channel

Substituting MGF expression (3.28) of Rayleigh fading channel, (4.5) becomes,

$$\bar{P}_b = \frac{1}{\pi}\int_0^{\frac{\pi}{2}} \frac{1}{1+\frac{\bar{\gamma}}{\sin^2\theta}} d\theta. \tag{4.6}$$

This integration is further modified as follows:

$$\begin{aligned}\bar{P}_b &= \frac{1}{\pi}\int_0^{\frac{\pi}{2}} \left(1 - \frac{\bar{\gamma}}{\bar{\gamma}+\sin^2\theta}\right) d\theta \\ &= \frac{1}{2} - \frac{\bar{\gamma}}{\pi}\int_0^{\frac{\pi}{2}} \frac{1}{\bar{\gamma}+\sin^2\theta} d\theta.\end{aligned} \tag{4.7}$$

Here we can apply the indefinite integral given in [29, eqn 2.562.1]:

$$\int \frac{dx}{a+b\sin^2 x} = \frac{1}{\sqrt{a(a+b)}} \arctan\left(\sqrt{\frac{a+b}{a}}\tan x\right), \quad \text{for } a>0 \tag{4.8}$$

By combining (4.7) and (4.8), we obtain

$$\bar{P}_b = \frac{1}{2}\left(1 - \sqrt{\frac{\bar{\gamma}}{\bar{\gamma}+1}}\right). \tag{4.9}$$

Rician Fading Channel

Let us substitute the Rician fading channel MGF expression (3.34) into (4.5), then we get

$$\bar{P}_b = \frac{1}{\pi}\int_0^{\frac{\pi}{2}} \frac{(K+1)\sin^2\theta}{(K+1)\sin^2\theta+\bar{\gamma}} \exp\left(-\frac{K\bar{\gamma}}{(K+1)\sin^2\theta+\bar{\gamma}}\right) d\theta. \tag{4.10}$$

The integration in (4.10) does not admit closed-form solution.

Nakagami Fading Channel

MGF for Nakagami fading channel is given in equation (3.38). When it is combined with (4.5), we obtain

$$\bar{P}_b = \frac{1}{\pi}\int_0^{\frac{\pi}{2}} \left(\frac{\sin^2\theta}{\sin^2\theta+c}\right)^m d\theta, \tag{4.11}$$

where $c = \frac{\bar{\gamma}}{m}$. This integral has the same form with the integral computed in Appendix 5A of [25]. Using the result, (4.11) becomes,

$$\bar{P}_b = \begin{cases} \frac{1}{2}\left[1 - \sqrt{\frac{\bar{\gamma}}{m+\bar{\gamma}}} \sum_{k=0}^{m-1} \binom{2k}{k} \left(\frac{m}{4(m+\bar{\gamma})}\right)^k\right], & m \text{ integer} \\ \frac{1}{2\sqrt{\pi}} \frac{\sqrt{\frac{\bar{\gamma}}{m}}}{\left(1+\frac{\bar{\gamma}}{m}\right)^{m+\frac{1}{2}}} \frac{\Gamma(m+\frac{1}{2})}{\Gamma(m+1)} \, {}_2F_1\left(1, m+\frac{1}{2}; m+1; \frac{m}{m+\bar{\gamma}}\right), & \text{otherwise} \end{cases} \tag{4.12}$$

where ${}_2F_1(\cdot,\cdot;\cdot;\cdot)$ is the Gauss hypergeometric function [4, eqn 15.1.1].

Weibull Fading Channel

To the best of the author's knowledge, general closed form MGF of a Weibull random variable is not available in literature. Though we can proceed computing (4.5) with the MGF expressions which are given in [16], [17] and [18] for an integer or rational shape parameter, yet, the resulting formulas will contain integrals that cannot be computed in closed form. Therefore, for further BEP analysis for a Weibull fading channel has been omitted.

Numerical results for the average BEP expressions of AWGN channel, Rayleigh, Rician, and Nakagami fading channels, equations (4.1), (4.9), (4.10), and (4.12), respectively, are depicted in Figure 4.1.

4.2 Outage Probability and Outage Capacity

Fading channels are characterized by rapidly changing channel. On the other hand, acceptable communication typically calls for a minimum threshold signal level. Therefore, outage probability P_{out} is one of the most common performance measures in wireless communication systems. It is defined as the probability that the system SNR falls below a certain quality of service threshold, ϵ:

$$P_{out} = P\{\gamma < \epsilon\} = \int_0^{\epsilon} f_\gamma(x)dx = F_\gamma(\epsilon). \tag{4.13}$$

Note from (4.13) that the outage probability is the cumulative distribution function of γ evaluated at ϵ. Therefore, using CDF expressions (3.27), (3.33), (3.37), and (3.41) for Rayleigh, Rician, Nakagami, and Weibull fading channels, respectively, we can get the corresponding fading channel outage

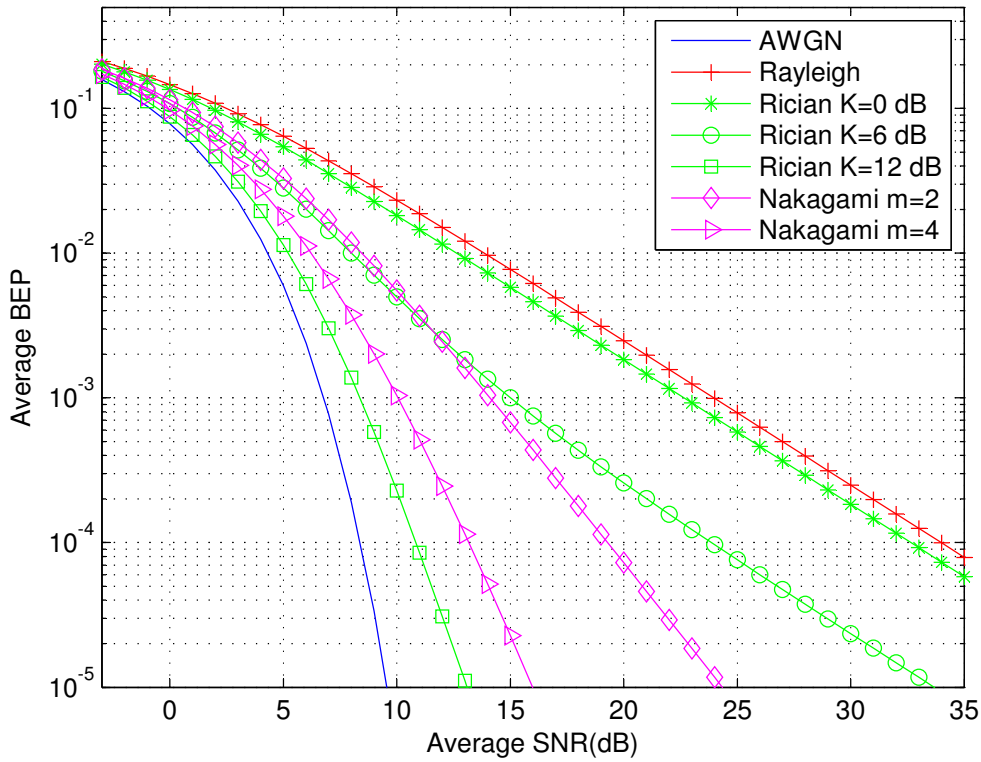

Figure 4.1: Average BEP versus average SNR of BPSK in AWGN, Rayleigh, Rician ($K = 0$ dB, 6 dB, 12 dB) and Nakagami ($m = 2, m = 4$) channels

probability expressions. The resulting expressions are given as follows. For Rayleigh fading channel, it is found that

$$P_{out} = F_\gamma(\epsilon) = 1 - \exp\left(-\frac{\epsilon}{\bar{\gamma}}\right), \tag{4.14}$$

and for Rician fading channel, we have

$$P_{out} = F_\gamma(\epsilon) = 1 - Q_m\left(\sqrt{2K}, \sqrt{\frac{2(K+1)\epsilon}{\bar{\gamma}}}\right). \tag{4.15}$$

Furthermore, for Nakagami fading channel,

$$P_{out} = F_\gamma(\epsilon) = \frac{\Gamma(m, \frac{m\epsilon}{\bar{\gamma}})}{\Gamma(m)}, \tag{4.16}$$

and for Weibull fading channel,

$$P_{out} = F_{\gamma}(\epsilon) = 1 - \exp\left[-\left(\frac{\epsilon}{b\bar{\gamma}}\right)^{\frac{\beta}{2}}\right], \tag{4.17}$$

where $b = 1/\Gamma\left(1 + \frac{2}{\beta}\right)$.

Outage capacity, which we denote by $C(P_{out})$, has been defined as the maximal transmission rate for a given outage probability and it is calculated as

$$C(P_{out}) = \text{BW} \cdot \log_2(1 + \epsilon(P_{out})) \tag{4.18}$$

where BW is the bandwidth of the system and $\epsilon(P_{out})$ is the value of SNR which is calculated from (4.14), (4.15), (4.16), or (4.17) for a given outage probability P_{out}. Note that $\epsilon(.)$ is the inverse of CDF and it usually does not admit a closed-form expression but is calculated numerically.

4.3 Average Capacity

Channel capacity defines the maximum data rate that can be sent over the channel with asymptotically small error probability. It represents an optimistic upper bound for practical communication schemes; therefore, it serves as a benchmark against which to compare the spectral efficiency of all practical transmission schemes. Based on available information at the transmitter and receiver about the time-varying channel and type of adaptive transmission policy used by the transmitter, various definitions are used to calculate capacity of flat fading channel [30, 31, 32]. We will follow the definition of capacity in case the transmitter cannot adapt its transmission strategy relative to the channel fade information which is available at only the receiver. Given that BW is the bandwidth of the system, Ergodic capacity is obtained by averaging the capacity of an AWGN channel. Therefore, AWGN channel capacity, denoted by C^{AWGN}, and average capacity, denoted by C, are formulated, respectively as follows:

$$C^{AWGN} = \text{BW} \cdot \log_2(1 + \gamma), \tag{4.19}$$

$$C = \int_0^\infty \mathrm{BW} \cdot \log_2(1+\gamma) f_\gamma(\gamma) d\gamma. \tag{4.20}$$

With the help of the logarithmic identity $\log_a(b) = \frac{\log_c(b)}{\log_c(a)}$, equation (4.20) is simplified into form

$$C = \frac{\mathrm{BW}}{\ln(2)} \int_0^\infty \ln(1+\gamma) f_\gamma(\gamma) d\gamma. \tag{4.21}$$

Rayleigh Fading Channel

Substituting PDF expression of Rayleigh fading channel given in (3.26) into (4.21), we find that

$$C = \frac{\mathrm{BW}}{\ln(2)\bar{\gamma}} \int_0^\infty \ln(1+\gamma) \exp\left(-\frac{\gamma}{\bar{\gamma}}\right) d\gamma \tag{4.22}$$

Performing change of integration variable to $y = 1+\gamma$, Equation (4.22) is reduced into

$$C = \frac{\mathrm{BW}}{\ln(2)\bar{\gamma}} \exp\left(\frac{1}{\bar{\gamma}}\right) \int_1^\infty \ln(y) \exp\left(-\frac{y}{\bar{\gamma}}\right) dy \tag{4.23}$$

Then using the integration

$$\int_1^\infty e^{-\mu x} \ln(x) dx = -\frac{1}{\mu} \cdot \mathrm{Ei}(-\mu), \qquad [29, \text{eqn } 4.331.2] \tag{4.24}$$

Equation (4.23) becomes

$$C = -\frac{\mathrm{BW}}{\ln(2)} \exp\left(\frac{1}{\bar{\gamma}}\right) \mathrm{Ei}\left(-\frac{1}{\bar{\gamma}}\right), \tag{4.25}$$

where $\mathrm{Ei}(\cdot)$ is the exponential integral function, defined in [29, eqn 8.211.1] as

$$\mathrm{Ei}(x) = -\int_{-x}^\infty \frac{e^{-t}}{t} dt = \int_{-\infty}^x \frac{e^t}{t} dt. \tag{4.26}$$

Further discussion about average capacity in Rayleigh Fading channel can be found from [32] and [33].

Rician Fading Channel

Making use of the PDF of γ from (3.32), (4.21) is simplified for Rician fading channel into

$$C = \frac{\mathrm{BW}}{\ln(2)} \int_0^\infty \ln(1+\gamma) \frac{(1+K)e^{-K}}{\bar{\gamma}} \exp\left(-\frac{(1+K)\gamma}{\bar{\gamma}}\right) \times I_0\left(\sqrt{\frac{4K(1+K)\gamma}{\bar{\gamma}}}\right) d\gamma. \tag{4.27}$$

To the best knowledge of the author, this integral does not have closed-form expression, but [33] and [34] give clear methods to express it in an infinite series form. The expression which is given in [34] is

$$C = \frac{\mathrm{BW}}{\ln(2)} \frac{(1+K)e^{-K}}{\bar{\gamma}} \sum_{n=0}^{\infty} \frac{1}{(n!)^2} \left[\frac{K(1+K)}{\bar{\gamma}}\right]^n \times G_{2,3}^{3,1}\left[\frac{K+1}{\bar{\gamma}} \middle| \begin{matrix} -1-n, & -n \\ 0, & -1-n, \quad -1-n \end{matrix}\right], \tag{4.28}$$

where Meijer's G-function $G_{p,q}^{m,n}(\cdot)$ definition is given in [29, eqn 9.301].

Nakagami Fading Channel

Using the PDF expression in (3.36), Equation (4.21) is reduced into form

$$C = \frac{\mathrm{BW} m^m}{\ln(2)\bar{\gamma}^m \Gamma(m)} \int_0^\infty \gamma^{m-1} \ln(1+\gamma) e^{-\frac{m\gamma}{\bar{\gamma}}} d\gamma. \tag{4.29}$$

For integer m, the integration in (4.29) is solved in Appendix B of [32]. Using the result from there and the identity $\Gamma(m) = (m-1)!$ for an integer m, (4.29) becomes

$$C = \frac{\mathrm{BW}}{\ln(2)} e^{\frac{m}{\bar{\gamma}}} \sum_{k=1}^{m} \left(\frac{m}{\bar{\gamma}}\right)^{m-k} \Gamma\left(-m+k, \frac{m}{\bar{\gamma}}\right), \tag{4.30}$$

where $\Gamma(\cdot,\cdot)$ is the incomplete gamma function which is defined as

$$\Gamma(\alpha, x) = \int_x^\infty e^{-t} t^{\alpha-1} dt. \qquad [29, \text{eqn } 8.350.2] \tag{4.31}$$

Making change of summation parameter such that $l = m - k$,

$$C = \frac{\text{BW}}{\ln(2)} e^{\frac{m}{\bar{\gamma}}} \sum_{l=0}^{m-1} \left(\frac{m}{\bar{\gamma}}\right)^l \Gamma\left(-l, \frac{m}{\bar{\gamma}}\right). \tag{4.32}$$

Furthermore, reference [34] has formulated a closed form expression for C when m is arbitrary. The expression is presented as follows:

$$C = \frac{\text{BW}}{\ln(2)} \frac{1}{\Gamma(m)} \left(\frac{m}{\bar{\gamma}}\right)^m G_{2,3}^{3,1}\left[\frac{m}{\bar{\gamma}}\middle|\begin{matrix} & -m, & 1-m \\ 0, & -m, & -m \end{matrix}\right]. \tag{4.33}$$

Detailed analysis of channel capacity for Nakagami fading channel is presented in [35].

Weibull Fading Channel

We follow the same procedure for Weibull fading channel as we used for previous channels. Thus, substituting (3.40) into (4.21), we get

$$C = \frac{\text{BW} \cdot \beta}{2\ln(2)(b\bar{\gamma})^{\frac{\beta}{2}}} \int_0^\infty \gamma^{\frac{\beta}{2}-1} \ln(1+\gamma) \exp\left[-(b\bar{\gamma})^{-\frac{\beta}{2}} \gamma^{\frac{\beta}{2}}\right] d\gamma. \tag{4.34}$$

Equation (4.34) has been solved and expressed in closed form in terms of Meijer's G-functions in [36] and it is presented here as follows:

$$C = \frac{\beta(b\bar{\gamma})^{\frac{-\beta}{2}}}{2\ln(2)} \frac{\text{BW}\sqrt{k} l^{-1}}{(2\pi)^{\frac{k+2l-3}{2}}} G_{2l,k+2l}^{k+2l,l}\left[\frac{(b\bar{\gamma})^{-\frac{\beta k}{2}}}{k^k}\middle|\begin{matrix} & I(l,-\frac{\beta}{2}), & I(l,1-\frac{\beta}{2}) \\ I(k,0), & I(l,-\frac{\beta}{2}), & I(l,-\frac{\beta}{2}) \end{matrix}\right], \tag{4.35}$$

where

$$I(n,\xi) \triangleq \frac{\xi}{n}, \frac{\xi+1}{n}, \ldots, \frac{\xi+n-1}{n}, \tag{4.36}$$

ξ is an arbitrary real value and n is a positive integer. Moreover, $\frac{l}{k} = \frac{\beta}{2}$ where k and l are positive integers. Depending up on the value of β, a set with minimum values of k and l can be properly chosen (e.g., for $\beta = 1.4$ we have to choose $k = 10$ and $l = 7$).

Numerical results based on the expressions (4.19), (4.25), (4.28), (4.32), and (4.35) are shown in Figure 4.2. Only small number of terms are significant in case of the Rician infinite series average capacity expression. For instance, the expression converges with only the first 10 terms for $K = 3$ dB and $K = 6$ dB within the considered average SNR range (0 dB-25 dB). Anyhow the first 50 terms are used to generate the numerical result.

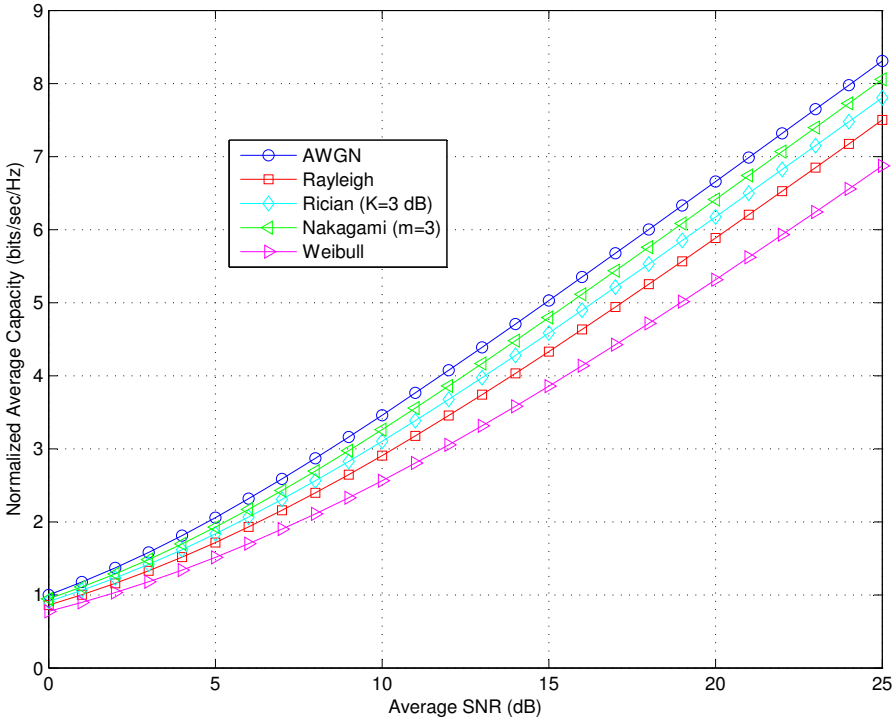

Figure 4.2: Normalized average capacity versus average SNR in AWGN, Rayleigh, Rician ($K = 3$ dB, $N = 50$), Nakagami ($m = 3$), and Weibull ($\beta = 1.4$) channels

Chapter 5

Analysis of Co-channel Interference

In this Chapter, the outage probability and average capacity of Rician/Rayleigh fading environment are computed and discussed. In Rician/Rayleigh fading environment, the *desired signal experiences Rician fading channel and the interfering signals experience Rayleigh fading channels*. Investigation of the scenario is important since it is highly probable that we face it in the future heterogeneous networks. In the first section, we cover revision of previous works on co-channel interference (CCI). The second section deals with Rician/Rayleigh scenario and its motivation. Then outage probability and average capacity computations and discussions are carried out for single interferer scenario in the following sections. Two expressions are found and presented for the outage probability: closed-form and infinite series expression. For average capacity an infinite series expression is found. Finally there is a section which describes how we can extend the results of the single interferer scenario into multi-interferer scenario.

5.1 Overview of Co-channel Interference Investigation

Large subscriber capacity and efficient use of spectrum are usually among the main objectives of cellular network design. Since the frequency spectrum

available for use in a cellular mobile radio system is limited, frequency reuse is an important feature to meet the objectives. The problem with reusing frequency band over relatively short distances is that co-channel interference is likely to occur. Though frequency reuse schemes of cellular systems are designed so that the interference between cells is minimized, CCI is always challenge. In the process of an improvement of capacity and coverage, small cells (femto cells and relay nodes) are being introduced in the conventional cellular networks. Hence CCI is continued to be seen as a major problem also in future cellular networks.

There have been extensive studies performed on CCI effects on the performance of the conventional macrocellular mobile radio systems (e.g. [37, 38, 39]). The same statistical characteristics has been assumed for the desired and interfering signals, which is reasonable for large cell systems. Rayleigh, Nakagami, lognormal, and superimposed Rayleigh/lognormal or Nakagami/lognormal models have been used to describe the environment.

Microcellular radio systems' performance in the presence of CCI has been also investigated [40, 41, 42, 43]. The usual logical assumption in microcellular systems is that the desired and interfering signals experience different fading channels. Rician/Rayleigh [40, 42], Rician/Nakagami [42], Rayleigh/Rician [42], Nakagami/Rician [42], and Nakagami/Nakagami [41] fading scenarios has been considered in these studies.

Almost all of the studies in the cases of both macrocellular and microcellular systems show the effect of CCI based on outage probability analysis. References [40, 42] have also presented analytical and numerical results of outage probability in the same fading environment we are heading to, Rayleigh/Rician. The closed-form outage probability computation result that will be presented here is in agreement with the results of the references. An infinite series expression is also found for the outage probability in this work. Furthermore, we will present average capacity computation and discussion.

5.2 Rician/Rayleigh Fading Scenario

Relay nodes and femtocells are being considered as among the major solutions to meet the coverage and capacity requirements of future networks [44, 45]. The deployment of relay nodes and femtocells in the conventional network result in a heterogeneous network; furthermore, the introduction of the small cells comes with different new challenges and interference is one of those.

The interference scenarios and characteristics in a heterogeneous deployment can be significantly different than in a homogeneous deployment [44, 46]. In [46], the different interference scenarios that exist between macrocell and femtocell, and among femtocells are defined. Some examples of interference scenarios that exists in heterogeneous deployments are provided in [44]. We can learn from those scenarios that it is highly probable to have a situation where the desired signal experiences line-of-sight condition and the interfering signals experience non-line-of-sight condition in case of both uplink and downlink communication. Therefore, studying Rician/Rayleigh fading environment is important and it is in the focus of the Chapter from now onwards. We will consider single interferer scenario at the beginning because of two reasons. First, it is common to have only one strong interferer situations in heterogeneous deployment [47]; and second, it is straightforward to extend the results for multi-interferer scenarios. There will be a discussion on how we can extend the single interferer scenario results to the multi-interferer ones in the last section of the Chapter.

The single interferer scenario which is going to be analyzed is shown in Figure 5.1. Transmitter Tx_1 transmits the desired signal and transmitter Tx_2 transmits the interfering signal. As can be seen from the figure, the channel of the interfering signal is considered to have no dominant path. As a result, its amplitude is modeled with Rayleigh distribution. Whereas, the desired signal channel is considered to have a dominant path and hence its amplitude is modeled with Rician distribution. The two channels can be considered as independent since the distance between Tx_1 and Tx_2 is much more greater than the wavelength of carrier signals used.

Referring Figure 2.8 and equation (2.14), the scenario is modeled by Figure 5.2 and equation (5.1) which are given below.

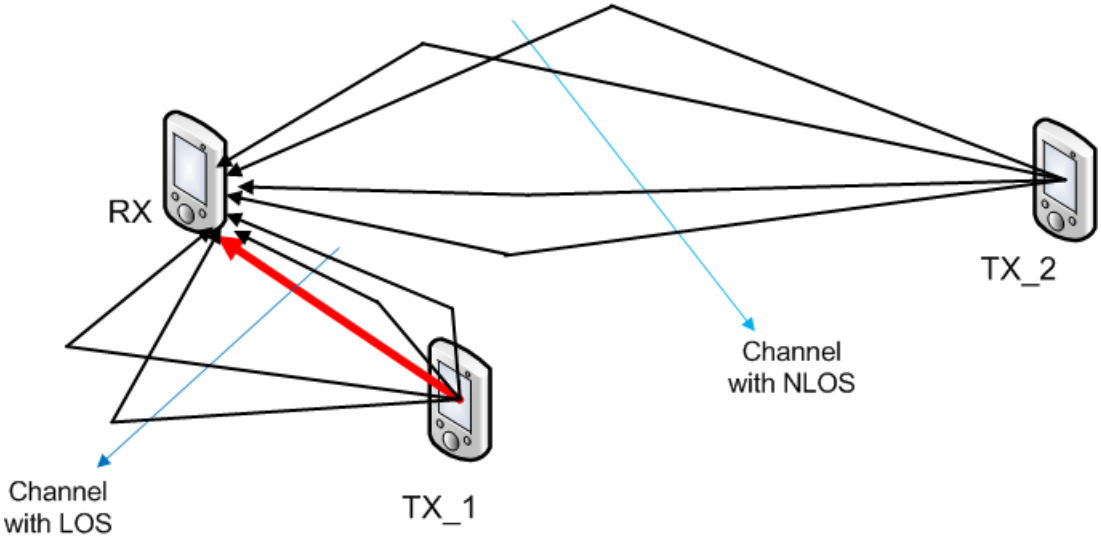

Figure 5.1: Rician/Rayleigh Scenario

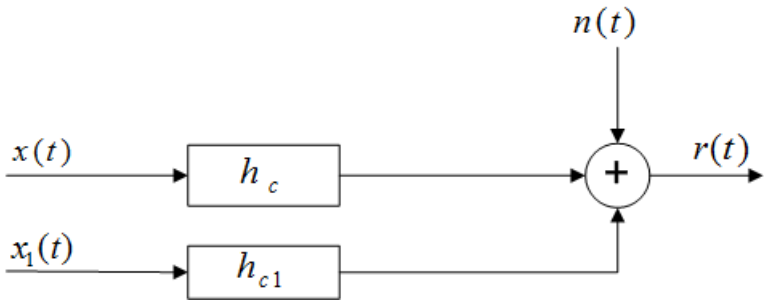

Figure 5.2: Link model in the presence of a single interfering transmitter

$$r(t) = h_c x(t) + h_{c1} x_1(t) + n(t). \tag{5.1}$$

where h_c and h_{c1} are the complex baseband channels of the desired and interfering signals, respectively, $x(t)$ and $x_1(t)$ are the transmitted desired and interfering signals, respectively, and $n(t)$ is additive white Gaussian noise.

In a system where we have both interference and noise channel impairments, signal to interference plus noise ratio (SINR) characterizes the performance of the system. Therefore, in our case, the SINR at the receiver, denoted by γ, is given below provided that P_{rx1}, P_{rx2} and P_n are the received desired signal

power, received interference power, and noise power, respectively:

$$\gamma = \frac{P_{rx1}}{P_n + P_{rx2}} = \frac{\gamma_1}{1+\gamma_2}, \tag{5.2}$$

where $\gamma_1 = \frac{P_{rx1}}{P_n}$ is the desired SNR and $\gamma_2 = \frac{P_{rx2}}{P_n}$ is the interference SNR.

The SNR γ_1 is affected by the Rician fading channel and the SNR γ_2 is affected by the Rayleigh fading channel in a way described by (3.21). PDF and CDF of γ_1 and γ_2 can be obtained from Chapter 3. Thus,

$$\begin{aligned} f_{\gamma_1}(\gamma) &= \frac{(1+K)e^{-K}}{\bar{\gamma}_1} \exp\left(-\frac{(1+K)\gamma}{\bar{\gamma}_1}\right) I_0\left(\sqrt{\frac{4K(1+K)\gamma}{\bar{\gamma}_1}}\right), \\ F_{\gamma_1}(\gamma) &= 1 - Q_m\left(\sqrt{2K}, \sqrt{\frac{2(K+1)\gamma}{\bar{\gamma}_1}}\right), \end{aligned} \tag{5.3}$$

where $\bar{\gamma}_1$ is the average of γ_1 and K is the Rician K factor. Furthermore,

$$f_{\gamma_2}(\gamma) = \frac{1}{\bar{\gamma}_2} e^{-\frac{\gamma}{\bar{\gamma}_2}}, \qquad F_{\gamma_2}(\gamma) = 1 - \exp\left(-\frac{\gamma}{\bar{\gamma}_2}\right), \tag{5.4}$$

where $\bar{\gamma}_2$ is the average of γ_2.

In the coming computations, we consider interference limited system which is a reasonable assumption for small cells. Therefore, we approximate the SINR as

$$\begin{aligned} \gamma = \frac{\gamma_1}{1+\gamma_2} &= \frac{\gamma_1}{\gamma_2} \cdot \frac{\gamma_2}{1+\gamma_2} \\ &= \frac{\gamma_1}{\gamma_2} \cdot \left(1 - \frac{1}{\gamma_2} + \left(\frac{1}{\gamma_2}\right)^2 - \cdots\right) \qquad \gamma_2 > 1 \\ &\cong \frac{\gamma_1}{\gamma_2} = \tilde{\gamma} \qquad \gamma_2 \gg 1. \end{aligned} \tag{5.5}$$

Here $\tilde{\gamma}$ is SIR and it is not only an approximation of SINR but also a tight upper bound. Consequently, the outage probability and average capacity results which we are going to compute using $\tilde{\gamma}$ will be a lower bound and an upper bound results, respectively.

5.3 Outage Probability

Using the definition given in the previous Chapter here by replacing γ with $\tilde{\gamma}$, outage probability for a certain quality of service threshold, ϵ, is

$$P_{out} = P\{\tilde{\gamma} < \epsilon\} = P\{\frac{\gamma_1}{\gamma_2} < \epsilon\}. \tag{5.6}$$

Since γ_1 and γ_2 are considered as independent, equation (5.6) reduces into a form,

$$P_{out} = 1 - P\{\frac{\gamma_1}{\epsilon} \geq \gamma_2\} = 1 - \int_0^\infty F_{\gamma_2}\left(\frac{x}{\epsilon}\right) f_{\gamma_1}(x)dx. \tag{5.7}$$

Substituting CDF of γ_2 from (5.4) in to the integral expression of (5.7) gives

$$P_{out} = 1 - \int_0^\infty \left[1 - \exp\left(-\frac{x}{\bar{\gamma}_2\epsilon}\right)\right] f_{\gamma_1}(x)dx. \tag{5.8}$$

Since, by definition,

$$\int_0^\infty f_{\gamma_1}(x)dx = 1, \tag{5.9}$$

equation 5.8 reduces into

$$P_{out} = \int_0^\infty \left[\exp\left(-\frac{x}{\bar{\gamma}_2\epsilon}\right)\right] f_{\gamma_1}(x)dx. \tag{5.10}$$

Substituting the PDF of γ_2 from equation (5.4) gives

$$P_{out} = \int_0^\infty \frac{(1+K)}{\bar{\gamma}_1} \exp\left(-K - \left(\frac{1}{\bar{\gamma}_2\epsilon} + \frac{(1+K)}{\bar{\gamma}_1}\right)x\right) \times I_0\left(\sqrt{\frac{4K(1+K)x}{\bar{\gamma}_1}}\right) dx. \tag{5.11}$$

Changing variable of integration in equation 5.11 to

$$y = \sqrt{\frac{2(\bar{\gamma}_1 + \bar{\gamma}_2(K+1)\epsilon)x}{\bar{\gamma}_1\bar{\gamma}_2\epsilon}}, \tag{5.12}$$

we have

$$x = \frac{\bar{\gamma}_1 \bar{\gamma}_2 \epsilon y^2}{2(\bar{\gamma}_1 + \bar{\gamma}_2(K+1)\epsilon}, \tag{5.13}$$

and

$$dx = \frac{\bar{\gamma}_1 \bar{\gamma}_2 \epsilon y}{(\bar{\gamma}_1 + \bar{\gamma}_2(K+1)\epsilon} dy. \tag{5.14}$$

Then equation 5.11 becomes

$$\begin{aligned} P_{out} =& \frac{\bar{\gamma}_2(K+1)\epsilon}{\bar{\gamma}_1 + \bar{\gamma}_2(K+1)\epsilon} \int_0^\infty y \exp\left[-\left(K + \frac{y^2}{2}\right)\right] \\ & \times I_0\left(\sqrt{\frac{2\bar{\gamma}_2 K(K+1)\epsilon}{\bar{\gamma}_1 + \bar{\gamma}_2(K+1)\epsilon}} y\right) dy. \end{aligned} \tag{5.15}$$

Addition and subtraction of $\frac{\bar{\gamma}_2 K(K+1)\epsilon}{\bar{\gamma}_1 + \bar{\gamma}_2(K+1)\epsilon}$ in the argument of the exponential expression in (5.15), and rearrangement of terms gives

$$\begin{aligned} P_{out} =& \frac{\bar{\gamma}_2(K+1)\epsilon}{\bar{\gamma}_1 + \bar{\gamma}_2(K+1)\epsilon} \exp\left(\frac{-K\bar{\gamma}_1}{\bar{\gamma}_1 + \bar{\gamma}_2(K+1)\epsilon}\right) \\ & \int_0^\infty y \exp\left[-\left(\frac{\frac{2\bar{\gamma}_2 K(K+1)\epsilon}{\bar{\gamma}_1 + \bar{\gamma}_2(K+1)\epsilon}}{2} + y^2\right)\right] I_0\left(\sqrt{\frac{2\bar{\gamma}_2 K(K+1)\epsilon}{\bar{\gamma}_1 + \bar{\gamma}_2(K+1)\epsilon}} y\right). \end{aligned} \tag{5.16}$$

Then by mapping the integral using the definition of generalized Marcum function given in (3.13), we obtain

$$\begin{aligned} P_{out} =& \frac{\bar{\gamma}_2(K+1)\epsilon}{\bar{\gamma}_1 + \bar{\gamma}_2(K+1)\epsilon} \exp\left(\frac{-K\bar{\gamma}_1}{\bar{\gamma}_1 + \bar{\gamma}_2(K+1)\epsilon}\right) \\ & \times Q_1\left(\sqrt{\frac{2\bar{\gamma}_2 K(K+1)\epsilon}{\bar{\gamma}_1 + \bar{\gamma}_2(K+1)\epsilon}}, 0\right). \end{aligned} \tag{5.17}$$

In [25, eqn 4.23], the following identity is given:

$$Q_1(\alpha, 0) = 1 \qquad \alpha \geq 0 \tag{5.18}$$

Therefore,

$$P_{out} = \frac{\bar{\gamma}_2(K+1)\epsilon}{\bar{\gamma}_1 + \bar{\gamma}_2(K+1)\epsilon} \exp\left(\frac{-K\bar{\gamma}_1}{\bar{\gamma}_1 + \bar{\gamma}_2(K+1)\epsilon}\right). \tag{5.19}$$

In addition to the closed-form expression given in Equation (5.19), the outage probability admits the following infinite series expression:

$$P_{out} = \sum_{n=0}^{\infty} \left[\frac{K^n}{n!} e^{-K} \right] I_{\left(\frac{(K+1)\bar{\gamma}_2\epsilon}{\bar{\gamma}_1+(k+1)\bar{\gamma}_2\epsilon}\right)}(1+n,1), \tag{5.20}$$

where $I_p(a,b)$ is the ratio of the incomplete beta function and complete beta function as defined in [29, eqn 8.392] (See A.3). The derivation of Equation (5.20) is based on the CDF of single noncentral F distribution and is given in Appendix A.

Both the closed-form and infinite series expressions are verified in Figure 5.3. The figure shows the simulated results and analytical results of outage probability for $\bar{\gamma}_1 = 25$ dB, $\bar{\gamma}_2 = 15$ dB, $K = 6$ dB. The simulation results are generated considering both SIR and SINR, and in both case the number of simulation samples taken is 10^5. The series expression of the outage probability is truncated to 501 first terms. Only two curves are visible in the figure. The two analytical results and the simulated result which considers the SIR are overlapped and give the bottom curve. The top curve represents the simulated result of outage probability which considers SINR. The difference between the two curves comes due to the interference limited system assumption and approximation. Though 500 is taken as an upper limit for the infinite series outage probability expression, the convergence comes much sooner for all instances checked.

Numerical results of outage probability and outage capacity are given in Figure 5.4, Figure 5.5, and Figure 5.6. It can be observed that the higher the average SNR ratio, the lower the outage probability; and the higher Rician K factor, the lower the outage probability. The figures also show that the difference of outage probability between different values of K increases when we increase the average SNR ratio. Therefore, in heterogeneous networks, where strong LOS is expected, assuming Rayleigh faded desired signal ($K = 0$) is highly probable to lead to wrong conclusions.

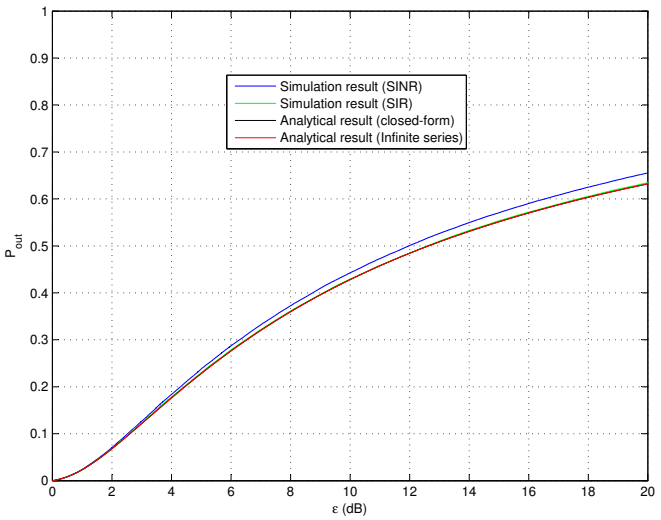

Figure 5.3: Outage probability versus threshold quality of service for simulated and analytical results

5.4 Average Capacity

The same definition of average capacity which is given in (4.20) is used here by replacing γ with $\tilde{\gamma} = \frac{\gamma_1}{\gamma_2}$:

$$C = \frac{\mathrm{BW}}{\ln(2)} \int_0^\infty \ln(1+\gamma) f_{\tilde{\gamma}}(\gamma) d\gamma. \tag{5.21}$$

Therefore, computing average capacity needs an expression for $f_{\tilde{\gamma}}(\gamma)$. Since γ_1 and γ_2 are considered independent, we get the following expression using [48, eqn 6-43]:

$$f_{\tilde{\gamma}}(\gamma) = \int_0^\infty y f_{\gamma_1}(\gamma y) f_{\gamma_2}(y) dy. \tag{5.22}$$

Using the PDF expressions in (5.3) and (5.4),

$$f_{\tilde{\gamma}}(\gamma) = \frac{(1+K)\exp(-K)}{\bar{\gamma}_1 \bar{\gamma}_2} \int_0^\infty y \exp\left(-\left(\frac{1}{\bar{\gamma}_2} + \frac{(1+K)\gamma}{\bar{\gamma}_1}\right) y\right) I_0\left(\sqrt{\frac{4K(K+1)\gamma y}{\bar{\gamma}_1}}\right) dy \tag{5.23}$$

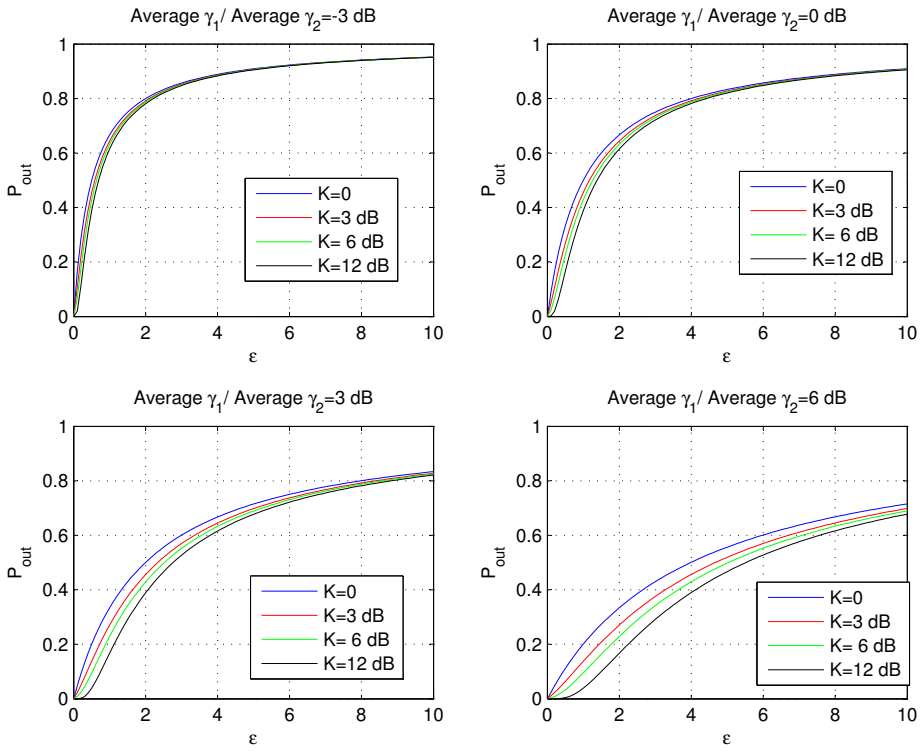

Figure 5.4: Outage probability versus threshold quality of service for different values of $\frac{\bar{\gamma}_1}{\bar{\gamma}_2}$

The integration is solved and $f_{\tilde{\gamma}}(\gamma)$ admits the following closed-form expression:

$$f_{\tilde{\gamma}}(\gamma) = \frac{(K+1)^3\bar{\gamma}_2^2\bar{\gamma}_1\gamma + (K+1)\bar{\gamma}_2\bar{\gamma}_1^2}{(\bar{\gamma}_1 + (K+1)\bar{\gamma}_2\gamma)^3} \exp\left(\frac{-K\bar{\gamma}_1}{\bar{\gamma}_1 + (K+1)\bar{\gamma}_2\gamma}\right). \qquad (5.24)$$

Though the PDF of $\tilde{\gamma}$ could be expressed with a closed-form expression as given in equation (5.24), equation (5.21) cannot be solved using this expression. Therefore, we proceed our computation by producing an infinite series expression for the PDF of $\tilde{\gamma}$.

Let $N_1 = \frac{1}{\bar{\gamma}_2} + \frac{(K+1)\gamma}{\bar{\gamma}_1}$ and $N_2 = \sqrt{\frac{4K(K+1)\gamma}{\bar{\gamma}_1}}$. Then using the series expression of $I_0(z)$,

$$I_0(z) = \sum_{n=0}^{\infty} \frac{\left(\frac{z}{2}\right)^{2n}}{(n!)^2}, \qquad [29, \text{eqn } 8.447.1] \qquad (5.25)$$

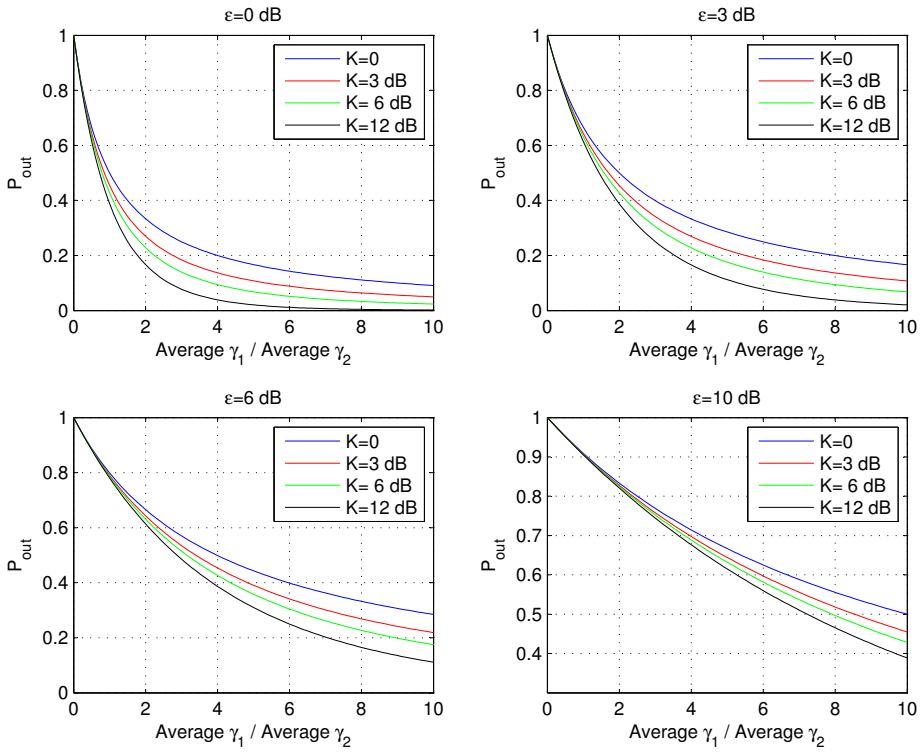

Figure 5.5: Outage probability versus $\frac{\bar{\gamma}_1}{\bar{\gamma}_2}$ for different values of threshold quality of service

and the integral

$$\int_0^\infty x^n e^{-\mu x} dx = n! \mu^{-n-1}, \qquad [29, \text{eqn } 3.351] \tag{5.26}$$

$f_{\tilde{\gamma}}(\gamma)$ reduces into an infinite series expression of the form,

$$f_{\tilde{\gamma}}(\gamma) = \frac{(1+K)\exp(-K)}{\bar{\gamma}_1 \bar{\gamma}_2} \sum_{n=0}^{\infty} \frac{\left(\frac{1}{4}N_2^2\right)^n}{n!} (n+1) N_1^{-n-2}. \tag{5.27}$$

Substituting (5.27) into (5.21) gives

$$C = \frac{\text{BW}}{\ln(2)} \frac{(1+K)\exp(-K)}{\bar{\gamma}_1 \bar{\gamma}_2} \sum_{n=0}^{\infty} \frac{n+1}{n!} \int_0^\infty \frac{\left(\frac{1}{4}N_2^2\right)^n}{N_1^{n+2}} \ln(1+\gamma) d\gamma \tag{5.28}$$

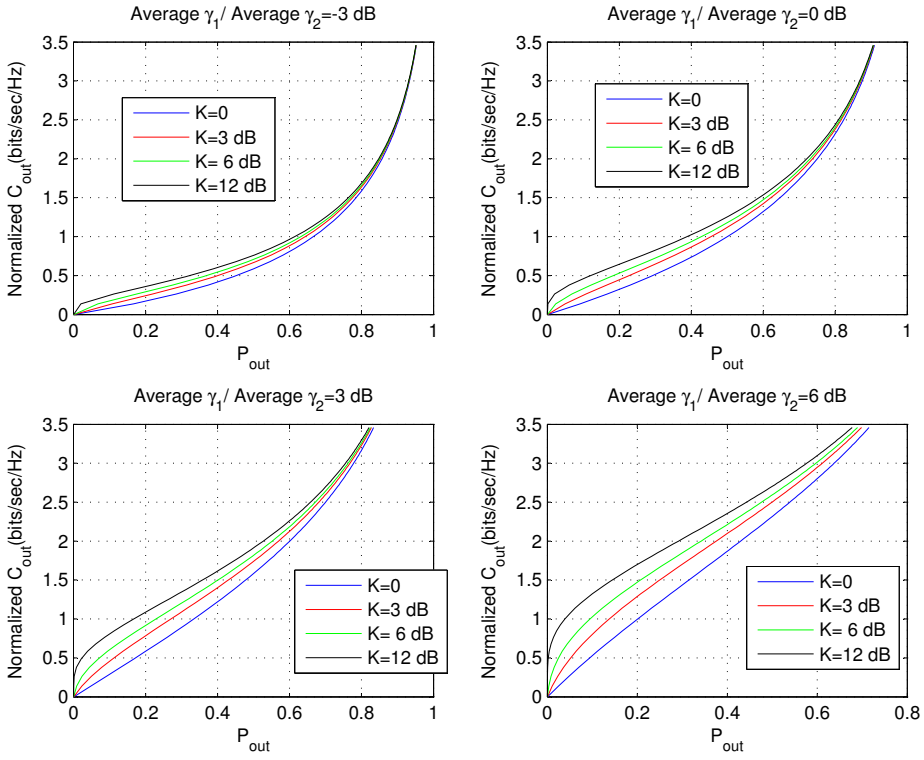

Figure 5.6: Outage capacity versus outage probability for different values of $\frac{\bar{\gamma}_1}{\bar{\gamma}_2}$

By replacing N_1 and N_2 with their corresponding expressions, we get

$$\begin{aligned} C &= \frac{\mathrm{BW}}{\ln(2)} \frac{(1+K)\exp(-K)}{\bar{\gamma}_1\bar{\gamma}_2} \sum_{n=0}^{\infty} \frac{n+1}{n!} \left(\frac{K(K+1)}{\bar{\gamma}_1}\right)^n \\ &\times \int_0^{\infty} \frac{\gamma^n \ln(1+\gamma)}{\left(\frac{1}{\bar{\gamma}_2} + \frac{(K+1)\gamma}{\bar{\gamma}_1}\right)^{n+2}} d\gamma \\ &= \frac{\mathrm{BW}}{\ln(2)} \frac{\exp(-K)}{\bar{\gamma}_2} \sum_{n=0}^{\infty} \frac{(n+1)K^n}{n!} \left(\frac{K+1}{\bar{\gamma}_1}\right)^{n+1} I_c, \end{aligned} \tag{5.29}$$

where

$$I_c = \int_0^{\infty} \frac{\gamma^n \ln(1+\gamma)}{\left(\frac{1}{\bar{\gamma}_2} + \frac{(K+1)\gamma}{\bar{\gamma}_1}\right)^{n+2}} d\gamma. \tag{5.30}$$

Let

$$a = \frac{1}{\bar{\gamma}_2} \text{ and } b = \frac{K+1}{\bar{\gamma}_1}. \tag{5.31}$$

Then by changing the variable of integration of I_c to $y = a + b\gamma$, we have $\gamma = \frac{y-a}{b}$ and $d\gamma = \frac{1}{b}dy$, and the integral reduces into a form

$$I_c = \int_a^\infty \frac{\left(\frac{y-a}{b}\right)^n \ln\left(1+\frac{y-a}{b}\right)}{by^{n+2}} dy. \tag{5.32}$$

Using binomial theorem [4, eqn 3.1.1],

$$\left(\frac{y-a}{b}\right)^n = \frac{1}{b^n}\sum_{k=0}^{n}\binom{n}{k}(-a)^{n-k}y^k. \tag{5.33}$$

After substituting (5.33) into (5.32) and rearranging terms, it can be found that

$$I_c = \frac{1}{b^{n+1}}\sum_{k=0}^{n}\binom{n}{k}(-a)^{n-k}\int_a^\infty y^{k-n-2}\ln\left(1+\frac{y-a}{b}\right)dy \tag{5.34}$$

An integration by parts and then the change of the variable of integration to $z = \frac{a}{y}$ gives

$$\int_a^\infty y^{k-n-2}\ln\left(1+\frac{y-a}{b}\right)dy = \frac{a^{k-n-1}}{n-k+1}\int_0^1 \frac{z^{n-k}}{1-\left(1-\frac{b}{a}\right)z}dz. \tag{5.35}$$

Using the integral in [4, eqn 15.3.1], it can be found that

$$\int_0^1 \frac{t^{n-k}}{1-st}dt = \frac{1}{n-k+1}\,{}_2F_1(1, n-k+1, n-k+2, s) \tag{5.36}$$

where ${}_2F_1(.,.;.;.)$ is the Gauss hypergeometric function [4, eqn 15.1.1]. Therefore, (5.35) becomes

$$\begin{aligned}&\int_a^\infty y^{k-n-2}\ln\left(1+\frac{y-a}{b}\right)dy \\ &= \frac{a^{k-n-1}}{(n-k+1)^2}\,{}_2F_1\left(1, n-k+1, n-k+2, 1-\frac{b}{a}\right).\end{aligned} \tag{5.37}$$

Then substituting (5.37) into (5.34) gives,

$$I_c = \frac{1}{ab^{n+1}} \sum_{k=0}^{n} \binom{n}{k} \frac{(-1)^{n-k}}{(n-k+1)^2} \, {}_2F_1\left(1, n-k+1, n-k+2, 1-\frac{b}{a}\right). \quad (5.38)$$

In conclusion, substituting equation (5.38) into equation (5.29) and replacing a and b with their corresponding expressions, we get

$$C = \frac{\mathrm{BW}\exp(-K)}{\ln(2)} \sum_{n=0}^{\infty} \frac{(n+1)K^n}{n!} \sum_{k=0}^{n} \binom{n}{k} \frac{(-1)^{n-k}}{(n-k+1)^2} \times {}_2F_1\left(1, n-k+1, n-k+2, 1-\frac{(K+1)\bar{\gamma}_2}{\bar{\gamma}_1}\right). \quad (5.39)$$

The analytical result is verified by creating numerical results for the normalized Ergodic capacity definitions

$$\frac{C}{\mathrm{BW}} = \frac{1}{\ln(2)} \int_0^{100{,}000} \int_0^{100{,}000} \ln(1+\frac{\gamma_1}{\gamma_2}) f_{\gamma_1}(\gamma_1) f_{\gamma_2}(\gamma_2) d\gamma_1 d\gamma_2, \quad (5.40)$$

and

$$\frac{C}{\mathrm{BW}} = \frac{1}{\ln(2)} \int_0^{100{,}000} \int_0^{100{,}000} \ln(1+\frac{\gamma_1}{1+\gamma_2}) f_{\gamma_1}(\gamma_1) f_{\gamma_2}(\gamma_2) d\gamma_1 d\gamma_2, \quad (5.41)$$

as shown in Figure 5.7. As can be seen from the figure, the analytical result and the numerical result of equation (5.40), which considers SIR, fit well. The curve of the numerical results of equation (5.41) is below the curve for the analytical result. Thus, we can see that the analytical result is a tight upper bound as stated before due the approximation used.

Numerical result of the average capacity is given in Figure 5.8. The infinite series expression converges with the first 30 terms for $K = 12$ dB with in the considered range of average SNR ratio $(0-10)$. For $K = 6$ dB, $K = 3$ dB, and $K = -40$ dB, it converges only with the first 12, 8 and 1 terms with in the range. Anyhow, the reference numerical result has been generated using 100 terms.

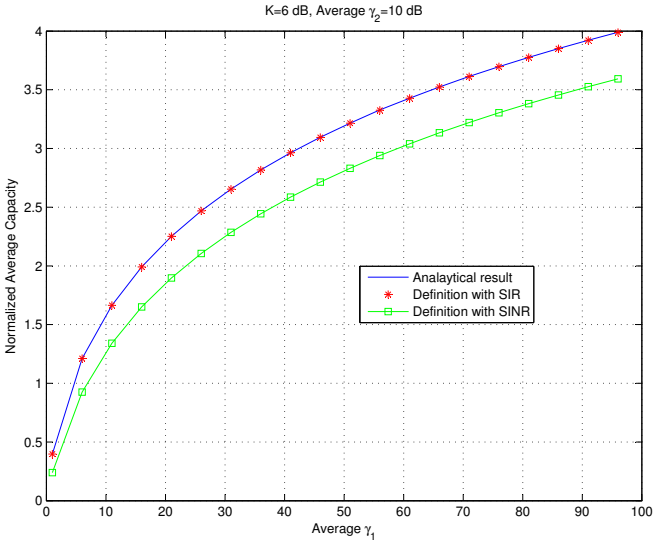

Figure 5.7: Normalized average capacity versus average of γ_1 for Ergodic capacity definition and analytical result

5.5 Extension of Single Interferer Case to Multi-interferer Case

When there are M interfering signals from neighbouring transceivers, the received signal is modeled as given in equation (2.14). It is assumed that each interfering signal SNR is corrupted by corresponding Rayleigh fading channel independently. This assumption is reasonable since the interfering signals transmitters are much far away from each other relative to the wavelength of the signals.

Let γ_1 be SNR of the desired Ricain signal and $\{\gamma_i : i = 2, 3, \ldots, M+1\}$ be SNRs of M independent Rayleigh interfering signals such that $f_{\gamma_i}(\gamma) = \frac{1}{\bar{\gamma}_i} \exp\left(-\frac{\gamma}{\bar{\gamma}_i}\right)$. Then the SINR is given and approximated as

$$\gamma = \frac{\gamma_1}{\sum_{i=2}^{M+1} \gamma_i + 1} \approx \frac{\gamma_1}{\sum_{i=2}^{M+1} \gamma_i} = \frac{\gamma_1}{S} = \tilde{\gamma}, \tag{5.42}$$

where $S = \sum_{i=2}^{M+1} \gamma_i$ and $\tilde{\gamma}$ is the SIR which is a tight upper bound for the SINR. Here, as in the case of single interferer scenario, the SIR $\tilde{\gamma}$ is used for the computation; hence, the resultant outage probability and average capacity

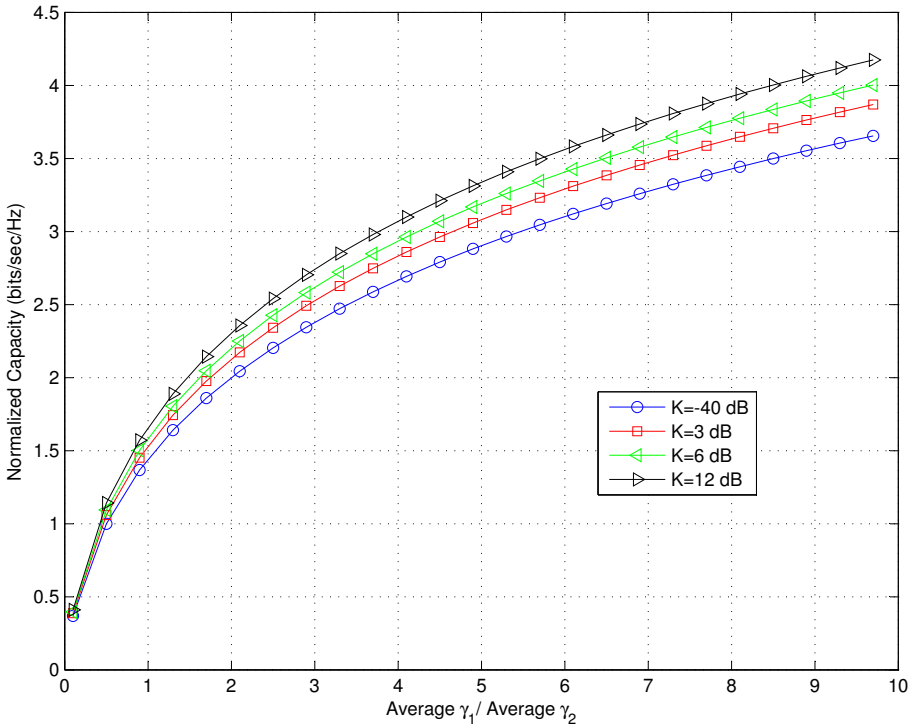

Figure 5.8: Normalized average capacity versus $\frac{\bar{\gamma}_1}{\bar{\gamma}_2}$

will be again tight lower bound and upper bound, respectively. The PDF of S is given by [49] when $\bar{\gamma}_i \neq \bar{\gamma}_j$ for $\forall\, i \neq j$:

$$f_S(\gamma) = \sum_{i=2}^{M+1} D_{i,M+1} \cdot \frac{1}{\bar{\gamma}_i} \exp\left(-\frac{\gamma}{\bar{\gamma}_i}\right) = \sum_{i=2}^{N+1} D_{i,N+1} f_{\gamma_i}(\gamma), \tag{5.43}$$

where $D_{i,M+1} = \prod_{j \neq i} \frac{\bar{\gamma}_i}{\bar{\gamma}_i - \bar{\gamma}_j}$. The CDF of S is obtained from (5.43) and is given as follows:

$$F_S(\gamma) = \int_0^{\gamma} f_S(t)dt = \sum_{i=2}^{M+1} D_{i,M+1} F_{\gamma_i}(\gamma). \tag{5.44}$$

5.5.1 Extension of Outage Probability

In case of multi-interferer, outage probability, denoted by P'_{out}, is given as

$$P'_{out} = P\{\tilde{\gamma} < \epsilon\} = 1 - \int_0^\infty F_S\left(\frac{x}{\epsilon}\right) f_{\gamma_1}(x)dx. \tag{5.45}$$

Substituting equation (5.44) gives,

$$P'_{out} = 1 - \sum_{i=2}^{M+1} D_{i,M+1} \int_0^\infty F_{\gamma_i}\left(\frac{x}{\epsilon}\right) f_{\gamma_1}(x)dx. \tag{5.46}$$

Then using equation (5.7), P'_{out} becomes

$$P'_{out} = 1 - \sum_{i=2}^{M+1} D_{i,M+1}\left[1 - P_{out}\right], \tag{5.47}$$

where P_{out} is the outage probability expression computed for a single interferer of γ_i. Therefore, utilizing the closed-form expression given by equation (5.19), we get

$$P'_{out}=1 - \sum_{i=2}^{M+1} D_{i,M+1}\left[1 - \frac{\bar{\gamma}_i(K+1)\epsilon}{\bar{\gamma}_1 + \bar{\gamma}_i(K+1)\epsilon} \exp\left(\frac{-K\bar{\gamma}_1}{\bar{\gamma}_1 + \bar{\gamma}_i(K+1)\epsilon}\right)\right]. \tag{5.48}$$

We can also get an infinite sum expression for the multi-interferer case using equation (5.20).

5.5.2 Extension of Average Capacity

The average capacity denoted by C' in case of multi-interferer is computed as

$$C' = \frac{\mathrm{BW}}{\ln(2)} \int_0^\infty \ln(1+\gamma) f_{\tilde{\gamma}}(\gamma)d\gamma. \tag{5.49}$$

Utilizing expression in [48, eqn 6-43], we get

$$f_{\tilde{\gamma}}(\gamma) = \int_0^\infty y f_{\gamma_1}(\gamma y) f_S(y)dy. \tag{5.50}$$

Then substituting equation (5.43), equation (5.50) reduces into a form

$$f_{\tilde{\gamma}}(\gamma) = \sum_{i=2}^{M+1} D_{i,M+1} f_{\gamma'}(\gamma). \tag{5.51}$$

where $\gamma' = \frac{\gamma_1}{\gamma_i}$. Finally, by using $f_{\tilde{\gamma}}(\gamma)$ expression in (5.51), equation (5.49) reduces into a form

$$C' = \sum_{i=2}^{M+1} D_{i,M+1} C, \tag{5.52}$$

where C is the average capacity computed for the single interferer case, given in Equation (5.39), in here $\bar{\gamma}_i$ replaces $\bar{\gamma}_2$.

The above analysis for extending single interferers expressions to multi-interferer ones are valid if and only if $\bar{\gamma}_i \neq \bar{\gamma}_j, \forall\, i \neq j$ with in the set $\{\gamma_i : i = 2, 3, \ldots, N+1\}$. Actually the validity of this condition is highly probable in practical heterogeneous cellular networks. On the other hand, the extension analysis admits complexity when $\bar{\gamma}_i = \bar{\gamma}_j$ for some or all different i and j. In this case, the sum of the interference SNRs follows Erlang distribution when all SNR's are equal or a different distribution whose PDF is computed in [50] when only some of them are equal.

Chapter 6

Conclusions

Heterogeneous networks are expected to improve coverage and capacity of future networks though there is additional interference challenges to be investigated. Therefore, understanding a heterogeneous network fading environments and the effects of co-channel interference is important for further measures such as mitigating the interference related problems. This work analyzes co-channel interference in Rician/Rayleigh fading scenario of heterogeneous network.

In the thesis, the first research question was to find the probability that a node of heterogeneous network is not able to reach a given quality of service requirement. A proper answer for this question is given in Chapter 5. Analytical and numerical results are presented for outage probability for the heterogeneous network fading scenario: Rician/Rayleigh. Two analytical expressions, closed-form and infinite sum, are found. We can deduce the following observations from the numerical results of outage probability in case of the single interferer scenario: the higher the Rician K factor, the lower the outage probability; the higher the ratio of the average SNRs, the lower the outage probability.

Finding maximum average transmission rate that we can achieve in a given radio link within a heterogeneous network was the second question aimed to be addressed. For the Rician/Rayleigh scenario, an infinite sum expression for average capacity is presented in Chapter 5, enabling us to answer the question in case of different parameter selections. Furthermore, the results help us to understand how much the strength of the dominant path of the desired signal

and co-channel interference affects the maximum average transmission rate achieved by a radio link.

Both the outage probability and average capacity expressions found and presented in this work are tight bounds. The reason for this is that we have approximated the SINR by its tight upper bound SIR throughout the analysis of both performance measures. Therefore, the outage probability result is a tight lower bound and the average capacity result is a tight upper bound of the corresponding results without the approximation.

Understanding properties of Gaussian, chi-square, Rayleigh, Rician, lognormal, Nakagami, and Weibull distribution are important to understand the statistical models of fading channels. In addition to their properties, the reasons why we apply the distributions have also been studied in Chapter 3. Furthermore, a thorough analysis of fading channel performance measures, including average BEP, in the absence of co-channel interference are covered in Chapter 4. Outage probability admits closed-form expression for Rayleigh, Rician, Nakagami and Weibull fading channel; whereas average BEP admits closed-form expression only for Rayleigh and Nakagami fading channel. Again average capacity has closed-form expressions for Rayleigh, Nakagami, and Weibull fading channel, and infinite sum expression for Rician fading channel.

In this work, we were concentrated on Rician/Rayleigh fading scenario. It is recommended to extend the analysis for the other fading channel models for both desired signal and interfering signals since the other models may also fit well depending on the environment. Understanding average BEP in the presence of co-channel interference is also relevant and has not discussed or analyzed here. In the analysis, the intention was always to attain a closed-form expressions primarily, and then, if the closed-form could not be found, to attain an infinite sum expression with fast convergence. This task required sometimes heavy mathematical tools. Therefore, in some cases, there is a possibility to come up with an alternative less complex and suitable expressions.

Bibliography

[1] L. Ahlin, J. Zander, and B. Slimane, *Principles of Wireless Communications.* Overseas Press India Private Ltd, 2006.

[2] J. G. Proakis and M. Salehi, *Digital Communications, 5th ed.* McGraw-Hill, 2008.

[3] S. Haykin, *Communication Systems*, 4th ed. New York, USA: John Wiley & Sons, 2001.

[4] M. Abramowitz and I. A. Stegun, *Handbook of Mathematical Functions with Formulas, Graphs, and Mathematical Tables*, ninth dover printing, tenth gpo printing ed. New York: Dover, 1964.

[5] K. Kim and G. Shevlyakov, "Why Gaussianity?" *IEEE Signal Processing Magazine*, vol. 25, no. 2, pp. 102–113, March 2008.

[6] M. Pätzold, *Mobile Fading Channels.* West Sussex, England: John Wiley & Sons, 2002.

[7] L. Johnson, S. Kotz, and N. Balakrishnan, *Continuous Univariate Distributions,Volume 1, 2nd ed.* John Wiley & Sons, 1995.

[8] J. Marcum, "A statistical theory of target detection by pulsed radar," *IRE Transactions on Information Theory*, vol. 6, no. 2, pp. 59–267, april 1960.

[9] J. Young, W.R., "Comparison of Mobile Radio Transmission at 150, 450, 900, and 3700 mc," *Transactions of the IRE Professional Group on Vehicular Communications*, vol. 3, no. 1, pp. 71–84, Jun 1953.

[10] H. Nylund, "Characteristics of Small-area Signal Fading on Mobile Circuits in the 150 MHz Band," *IEEE Transactions on Vehicular Technology*, vol. 17, no. 1, pp. 24–30, Oct 1968.

[11] Y. Okumara, T. Kawano, and K. Fukuda, "Field Strength and Its Variability in VHF and Land-mobile Services," *Rev. Elec. Commun. Lab*, vol. 16, pp. 825–873, 1968.

[12] S. O. Rice, "Statistical Properties of a Sine Wave Plus Random Noise," *Bell System Tech. J.*, vol. 27, pp. 109–157, 1948.

[13] J. D. Parsons, *Mobile Radio Propagation Channel, 2nd ed.* West Sussex, England: John Wiley & Sons, 2000.

[14] M. K. Simon, *Probability Distributions Involving Gaussian Random Variables*. New York, USA: Springer, 2002.

[15] H. Suzuki, "A Statistical Model for Urban Radio Propagation," *IEEE Transactions on Communications*, vol. 25, no. 7, pp. 673–680, Jul 1977.

[16] S. Nadarajah and S. Kotz, "On The Weibull MGF," *IEEE Transactions on Communications*, vol. 55, no. 7, pp. 1287–1287, july 2007.

[17] J. Cheng, C. Tellambura, and N. Beaulieu, "Performance of digital linear modulations on Weibull slow-fading channels," *IEEE Transactions on Communications*, vol. 52, no. 8, pp. 1265–1268, aug. 2004.

[18] ——, "Performance analysis of digital modulations on Weibull fading channels," *Vehicular Technology Conference, 2003. VTC 2003-Fall. 2003 IEEE 58th*, vol. 1, pp. 236 – 240 Vol.1, oct. 2003.

[19] . IEEE Vehicular Technology Society Committee on Radio Propagation, "Coverage Prediction for Mobile Radio Systems Operating in the 800/900 MHz frequency range," *IEEE Transactions on Vehicular Technology*, vol. 37, no. 1, pp. 3–72, Feb 1988.

[20] H. Hashemi, "The Indoor Radio Propagation Channel," *Proceedings of the IEEE*, vol. 81, no. 7, pp. 943–968, Jul 1993.

[21] G. Tzeremes and C. Christodoulou, "Use of Weibull Distribution for Describing Outdoor Multipath Fading," in *Antennas and Propagation Society International Symposium, 2002. IEEE*, vol. 1, 2002, pp. 232–235 vol.1.

[22] M.-J. Ho and G. Stuber, "Co-channel Interference of Microcellular Systems on Shadowed Nakagami Fading Channels," *Vehicular Technology Conference, 1993 IEEE 43rd*, pp. 568 –571, may 1993.

[23] A. Abdi and M. Kaveh, "K distribution: An Appropriate Substitute for Rayleigh-lognormal Distribution in Fading-shadowing Wireless Channels," *Electronics Letters*, vol. 34, no. 9, pp. 851 –852, apr 1998.

[24] P. Bithas, "Weibull-gamma Composite Distribution: Alternative Multipath/Shadowing Fading Model," *Electronics Letters*, vol. 45, no. 14, pp. 749–751, 2 2009.

[25] M. K. Simon and M.-S. Alouini, *Digital Communication over Fading Channels*. John Wiley & Sons, 2000.

[26] K. Cho and D. Yoon, "On the general BER expression of one- and two-dimensional amplitude modulations," *IEEE Transactions on Communications*, vol. 50, no. 7, pp. 1074–1080, jul 2002.

[27] K. Sankar, "Bit Error Rate for BPSK modulation," http://www.dsplog.com/2007/08/05/bit-error-probability-for-bpsk-modulation/, August 2007.

[28] J. Craig, "A New, Simple and Exact Result for Calculating the Probability of Error for Two-dimensional Signal Constellations," *Military Communications Conference, 1991. MILCOM '91, Conference Record, 'Military Communications in a Changing World'., IEEE*, pp. 571 –575 vol.2, nov 1991.

[29] A. Jeffrey and D. Zwillinger, *Gradshteyn and Ryzhik's Table of Integrals, Series and Products*. Elsevier, 2007.

[30] A. Goldsmith, *Wireless Communications*. Cambridge University Press, 2005.

[31] A. Goldsmith and P. Varaiya, "Capacity of fading channels with channel side information," *IEEE Transactions on Information Theory*, vol. 43, no. 6, pp. 1986–1992, nov 1997.

[32] M.-S. Alouini and A. Goldsmith, "Capacity of rayleigh fading channels under different adaptive transmission and diversity-combining techniques," *Vehicular Technology, IEEE Transactions on*, vol. 48, no. 4, pp. 1165 –1181, jul 1999.

[33] W. Lee, "Estimate of channel capacity in Raleigh fading environment," *Vehicular Technology Conference, 1988, IEEE 38th*, pp. 582 –584, jun 1988.

[34] N. Sagias, G. Tombras, and G. Karagiannidis, "New results for the Shannon channel capacity in generalized fading channels," *IEEE Communications Letters*, vol. 9, no. 2, pp. 97–99, feb. 2005.

[35] M.-S. Alouini and A. Goldsmith, "Capacity of Nakagami multipath fading channels," *Vehicular Technology Conference, 1997 IEEE 47th*, vol. 1, pp. 358 –362 vol.1, may 1997.

[36] N. Sagias, D. Zogas, G. Karagiannidis, and G. Tombras, "Channel capacity and second-order statistics in Weibull fading," *IEEE Communications Letters*, vol. 8, no. 6, pp. 377–379, june 2004.

[37] K. Sowerby and A. Williamson, "Outage probability calculations for multiple cochannel interferers in cellular mobile radio systems," *IEE Proceedings on Radar and Signal Processing*, vol. 135, no. 3, pp. 208–215, jun 1988.

[38] K. W. K. W. Sowerby, "Outage probability in mobile radio systems," Ph.D. dissertation, University of Auckland, New Zealand, 1989.

[39] Q. Zhang, "Outage probability in cellular mobile radio due to Nakagami signal and interferers with arbitrary parameters," *IEEE Transactions on Vehicular Technology*, vol. 45, no. 2, pp. 364 –372, may 1996.

[40] Y.-D. Yao and A. Sheikh, "Outage probability analysis for microcell mobile radio systems with cochannel interferers in Rician/Rayleigh fading environment," *Electronics Letters*, vol. 26, no. 13, pp. 864–866, june 1990.

[41] ——, "Investigations into cochannel interference in microcellular mobile radio systems," *IEEE Transactions on Vehicular Technology*, vol. 41, no. 2, pp. 114–123, may 1992.

[42] H.-C. Yang and M.-S. Alouini, "Closed-form formulas for the outage probability of wireless communication systems with a minimum signal power constraint," *IEEE Transactions on Vehicular Technology*, vol. 51, no. 6, pp. 1689–1698, nov 2002.

[43] W. Yan and Z. Hongbo, "Outage probability for microcellular mobile radio systems in Rician fading channels," in *CEEM 2000. Proceedings. Asia-Pacific Conference on Environmental Electromagnetics*, 2000, pp. 82 –85, 85/1.

[44] 3GPP-TR36.814, "Further advancements for E-UTRA: physical layer aspects (Release 9), V9.0.0," Available at: www.3gpp.org., Tech. Rep., March 2010.

[45] D. Knisely, T. Yoshizawa, and F. Favichia, "Standardization of femtocells in 3GPP," *IEEE Communications Magazine*, vol. 47, no. 9, pp. 68–75, september 2009.

[46] 3GPP-TR25.820, "3G Home NodeB Study Item Technical Report (Release 8), V8.2.0," Available at: www.3gpp.org., Tech. Rep., September 2008.

[47] M. Husso, J. Hämäläinen, R. Jäntti, J. Li, E. Mutafungwa, R. Wichman, and Z. Zheng, "Interference Suppression by Practical Transmit Beamforming Methods in Closed Femtocells," *EURASIP Journal on Wireless Communications and Networking*, April 2010.

[48] A. Papoulis, *Probability, Random Variables, and Stochastic Processes, 3rd ed.* McGraw-Hill, 1991.

[49] S. M. Ross, *Introduction to Probability Models, 5th ed.* Academic Press, 2000.

[50] H. V. Khuong and H.-Y. Kong, "General expression for PDF of a sum of independent exponential random variables," *IEEE Communications Letters*, vol. 10, no. 3, pp. 159–161, mar 2006.

[51] L. Johnson, S. Kotz, and N. Balakrishnan, *Continuous Univariate Distributions,Volume 2, 2nd ed.* John Wiley & Sons, 1995.

[52] G. Robertson, "Computation of the Noncentral F Distribution (CFAR)Detection," *IEEE Transactions on Aerospace and Electronic Systems*, vol. AES-12, no. 5, pp. 568–571, sept. 1976.

Appendix A

Infinite Series Outage Probability Expression

Assume that the variable γ_1 is a non-central chi-square random variable with two degrees of freedom, and parameters: $a = \sqrt{\frac{K\bar{\gamma}_1}{K+1}}$, $\sigma_1 = \sqrt{\frac{\bar{\gamma}_1}{2(K+1)}}$. Furthermore, assume that γ_2 is a central chi-square random variable with two degrees of freedom and parameter $\sigma_2 = \sqrt{\frac{\bar{\gamma}_2}{2}}$.

Let γ_1' and γ_2' are the unit variance chi-square definition correspondence of γ_1 and γ_2, respectively. Hence, using their relationship as described in (3.15),

$$\gamma = \frac{\gamma_1}{\gamma_2} = \frac{\sigma_1^2\gamma_1'}{\sigma_2^2\gamma_2'} = \frac{\bar{\gamma}_1}{(K+1)\bar{\gamma}_2}X \tag{A.1}$$

where $X = \frac{\gamma_1'}{\gamma_2'}$ which is the quotient of unit variance definition noncentral and central chi-square random variables.

It can be seen [51, 52] that X is a single noncentral F distributed random variable with two degree of freedom for both the noncentral and central chi-square random variables, and noncentral parameter $\lambda = \frac{a^2}{\sigma_1^2} = \frac{\frac{K\bar{\gamma}_1}{K+1}}{\frac{\bar{\gamma}_1}{2(K+1)}} = 2K$. In [51, eqn 30.10] and [52], the CDF of the noncentral F distributed random variable Y with v_1 degree of freedom for noncentral chi-square variable, v_2 degree of freedom for the central chi-square variable, and noncentral parameter

of λ is given:

$$F_Y(y/v_1, v_2, \lambda) = \sum_{n=0}^{\infty} \left[\frac{\left(\frac{1}{2}\lambda\right)^n}{n!} e^{-\frac{-\lambda}{2}} \right] I_{\left(\frac{v_1 y}{v_2 + v_1 y}\right)} \left(\frac{1}{2}v_1 + n, \frac{1}{2}v_2 \right) \tag{A.2}$$

where $I_p(\cdot, \cdot)$ is the ratio of the incomplete beta function and complete beta function as defined in [29, eqn 8.392]. It is given as follows:

$$I_x(p, q) = \frac{1}{B(p, q)} \int_0^x t^{p-1}(1-t)^{q-1} dt, \tag{A.3}$$

where $B(p, q) = \int_0^1 t^{p-1}(1-t)^{q-1} dt$. Therefore, using (A.2), the CDF of X can be written as

$$F_X(x/2, 2, 2K) = \sum_{n=0}^{\infty} \left[\frac{K^n}{n!} e^{-K} \right] I_{\left(\frac{x}{1+x}\right)} (1 + n, 1)\,. \tag{A.4}$$

Using Equation (A.1) and scaling properties of CDF, we can conclude that

$$P_{out} = F_\gamma(\epsilon) = F_X \left(\frac{(K+1)\bar{\gamma}_2}{\bar{\gamma}_1} \epsilon \right). \tag{A.5}$$

Finally combining (A.4) and (A.5), we get

$$P_{out} = \sum_{n=0}^{\infty} \left[\frac{K^n}{n!} e^{-K} \right] I_{\left(\frac{(K+1)\bar{\gamma}_2 \epsilon}{\bar{\gamma}_1 + (k+1)\bar{\gamma}_2 \epsilon}\right)} (1 + n, 1). \tag{A.6}$$